JOURNAL OF GEOPHYSICAL RESEARCH, VOL. 91, NO. B9, PAGES 9099–9123, AUGUST 10, 1986

Deglaciation-Induced Vertical Motion of the North American Continent and Transient Lower Mantle Rheology

W. R. PELTIER

Department of Physics, University of Toronto, Ontario, Canada

The last deglaciation event of the current ice age, which began approximately 18,000 years ago and ended about 7000 years ago, continues to exert a profound influence on the vertical motion of the solid earth in and surrounding the regions which were once ice covered. Observations of such vertical motions may be employed to constrain the radial viscoelastic structure of the planet and therefore to contribute in an important way to the understanding of geodynamic processes in general. In this paper both present-day rates of vertical motion as recorded on tide gauges and long time scale records of vertical motion as recorded in ^{14}C-controlled relative sea level histories are employed to refine previously constructed models of the radial viscoelastic structure. An interesting sidelight to this analysis is the demonstration that the lower mantle viscosity inferred from the vertical motion data could represent a transient rather than the steady state value, a fact which would help considerably to reconcile the small viscosity stratification required by the glacial rebound data with the large stratification which seems to be required by some recent analyses of the geoid height anomalies associated with internal density heterogeneity of the mantle which has been revealed by application of seismic tomographic techniques. A further product of these new analyses is obtained by the application of the glacial isostatic adjustment model to filter this signal from the secular trends of relative sea level observed on tide gauges from both the east and west coasts of the North American continent. These results may be important in the context of recently proposed scenarios of climatic change.

1. INTRODUCTION

Understanding the rheology of the earth's mantle is crucial to a large number of problems in geodynamics. On the shortest time scales characteristic of elastic body waves and elastic-gravitational free oscillations, the deviation of the rheology from perfect Hookean elasticity (the anelasticity) determines seismic attenuation and endows the normal modes with finite Q. On the longest time scales characteristic of the mantle convective circulation the magnitude of the "steady state" viscosity determines the rate at which mantle material will be caused to flow by a given superadiabatic radial temperature gradient. On "intermediate" time scales, such as that of the 10^5 year glaciation-deglaciation cycle which has characterized the past million years of the Pleistocene period, the mechanical response of the planet to the applied surface loads associated with individual ice sheets may involve both short time scale anelastic stress relaxation as well as relaxation associated with the steady state viscous response. As discussed by *Peltier et al.* [1981] and *Peltier* [1984*a*, *b*], the rheology of the mantle is known to be sufficiently complex as to require several different "viscosities" in order to completely characterize it, especially when one restricts the characterization to be a member of the class of models which is usually called linearly viscoelastic. The phenomenological diagram shown in Figure 1 illustrates the fundamental connection between the characteristic time scale of a given geodynamic process and the particular viscosity of the mantle to which it will be sensitive. The steady state viscosity ν_1 governs the thermal convection process, whereas the transient viscosity ν_2 (or transient viscosities ν_2 in the case of an absorption band) governs shorter time scale anelastic processes. Since the boundary between these two regions is unknown at present it is not entirely clear on a priori grounds whether the intermediate time scale process of glacial isostatic adjustment should see the transient or steady component of the viscosity spectrum.

Over the past decade, a considerable body of new work has been completed upon the old problem of glacial isostatic adjustment, motivated in part by interest in attempting to determine whether postglacial rebound data were sensitive to the steady state or transient component of the rheology. The work which began with *Peltier* [1974] was entirely based upon the application of a simple linearly viscoelastic Maxwell representation of the rheology. This analogue is based upon the assumption that the initial response of mantle material to an applied shear stress is Hookean elastic whereas the final response is Newtonian viscous. This model has now been applied to reconcile an enormous quantity of data associated with the glacial isostatic adjustment process, including postglacial variations of relative sea level [*Peltier and Andrews*, 1976; *Peltier*, 1976, 1982; *Clark et al.*, 1978; *Peltier et al.*, 1978; *Wu and Peltier*, 1983], the free air gravity anomalies found over present-day regions of land emergence [*Peltier*, 1980; *Peltier and Wu*, 1982; *Wu and Peltier*, 1983], and anomalies in earth rotation including the true wander of the rotation pole observed in the ILS path [*Peltier*, 1982; *Peltier and Wu*, 1982; *Wu and Peltier*, 1984] and the so-called nontidal component of the acceleration of rotation which was originally inferred through analyses of ancient eclipse data and which has recently been reconfirmed through analysis of laser ranging data to the LAGEOS satellite [*Peltier*, 1982, 1983; *Peltier and Wu*, 1983; *Yoder et al.*, 1983; *Rubincam*, 1984; *Wu and Peltier*, 1984]. The main product of these analyses, aside from the important demonstration that this large class of geophysical observations is explicable as comprising different signatures of the planet's response to the Pleistocene glaciation-deglaciation cycle, consists of the mantle viscosity profile which has been inferred on the basis of fitting the rheological model to the totality of the data. All of these data have been shown to be compatible with the same radial variation of steady state shear viscosity which is characterized by an upper mantle value close to 10^{21} Pa s and a lower mantle value

Paper number 5B5700.
0148-0227/86/005B-5700$05.00

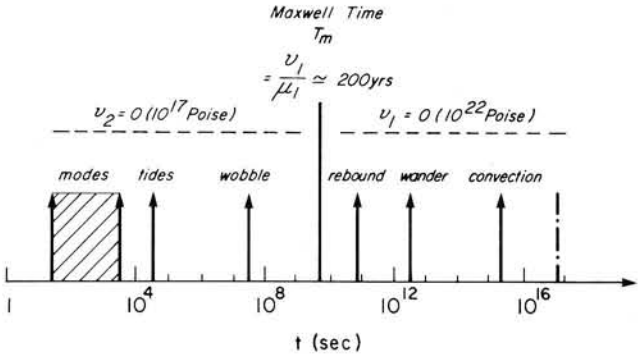

Fig. 1. Schematic diagram illustrating the characteristic time scale of several different geodynamic phenomena. Depending upon whether the characteristic time scale is long or short determines whether the phenomenon will see the transient or steady state components of the viscosity spectrum which are represented here as being characterized by the Burgher's body parameters ν_2 and ν_1, respectively. Note that the phenomenon of postglacial rebound is on the boundary separating these regimes.

somewhat higher, but modestly so, and close to the value of 3×10^{21} Pa s. Some of the rebound data have also been shown to be sensitive to continental lithospheric thickness and have been employed to constrain this parameter, in the case of the eastern part of the North American continent, to a value near 200 km [*Peltier*, 1984*a*, *b*].

When a Maxwell analogue is employed to characterize the rheology of the mantle, one is therefore led to conclude that the viscosity of this part of the earth is very nearly uniform and close to the value of 10^{21} Pa s. As pointed out by *Weertman* [1978], this result is somewhat at odds with expectations based upon microphysical models of the steady state creep process which are based upon the dynamics of dislocation climb, as well as with analyses of the increase of viscosity from the upper to the lower mantle expected on the basis of variations of creep activation energy and volume across the spinel → periclase phase transition at 670 km depth which separates the two regions [e.g., *Sammis et al.*, 1977]. *Weertman* [1978] first suggested that the way out of this impass was simply to assume that the low value of the viscosity inferred for the lower mantle from the rebound data was a transient rather than the steady state value (that is, was to be interpreted as a part of the ν_2 spectrum of Figure 1, rather than as the steady state value ν_1). Until rather recently, however, there was no observational evidence to support the notion that this idea was correct, and consequently, it remained equally probable that the microphysical models of the creep process where simply too poorly constrained to be applied to accurately deduce the expected viscosity profile. In fact, arguments reviewed by *Peltier* [1980, 1985*a*, *b*] based upon boundary layer theories of the mantle convection process have been advanced to show that if the steady state viscosity of the mantle were very much different than the value inferred from the glacial rebound data then it would be rather difficult to explain plate tectonic observations in terms of a thermal convection theory of continental drift.

Very recently some new evidence has appeared which does seem to very strongly support the interpretation of *Weertman* [1978]. This evidence consists of analyses of the large-scale structure of the planetary gravitational field by *Hager* [1984]. The work is based upon a Newtonian viscous parameterization of mantle rheology. Recent seismic tomographic inferences of the lateral heterogeneity of density existing in the mantle [*Dziewonski*, 1984; *Woodhouse and Dziewonski*, 1984] were employed to infer the flow which would be induced by the large-scale density heterogeneity. The geoid height anomaly which would be caused by the combined effects of the observed density heterogeneity and the boundary deformations associated with the induced flow was computed as a function of the viscosity contrast between the upper and lower mantle. The main result was the demonstration that very good fits to the observed low degree geoid height spectrum could be obtained but only if the viscosity of the lower mantle was very much higher than the viscosity of the upper mantle. Preferred models have an increase of viscosity by about a factor of 30 from the upper to the lower mantle. This is in very much closer accord with expectations based upon microphysical theories of the solid state creep process and very much at odds with the value of the lower mantle viscosity delivered by postglacial rebound analyses based upon the Maxwell analogue. One of the purposes of the present paper will be to show that the previous analyses of postglacial rebound using the Maxwell analogue are nevertheless liable to be perfectly accurate mechanical models of the rebound process if only the lower mantle viscosity inferred by application of it is interpreted as a transient value as *Weertman* [1978] first suggested. This is a rather important point (e.g., see Peltier [1985*c*]), since it would otherwise appear rather fortuitous that the large number of rebound observations cited previously have been reconciled by the same radial viscoelastic structure. The theoretical explanation of this fact will be provided in section 2. Although it may be rather premature to accept the results of *Hager* [1984] at face value, particular given the conflicting interpretations of closely related data by A. M. Forte and W. R. Peltier (unpublished manuscript, 1986), it is nevertheless important to realize that even if the result were correct it would not undermine the validity of the analyses of postglacial rebound phenomena which have already been completed with the Maxwell analogue and certainly not the theory which has been developed to do the required computations.

Following a discussion of this theoretical point in section 2 and a brief review of the model of postglacial relative sea level variation, the model will be employed to refine the picture of the radial viscoelastic structure which has been obtained in the course of previous analyses. Although the focus will be on the interpretation of vertical motion data from the North American continent, some further information will be provided concerning the rates of vertical motion which should be occurring today in northwestern Europe as a consequence of the continuing influence of glacial isostatic disequilibrium. Several data sets which have not previously been discussed from the point of view of their compatibility with the global model of isostatic adjustment will be integrated into the analysis and exploited to further constrain the properties of the stratification to which they are most sensitive. These new data sets include strandline tilts in the Great Lakes which mark the Lake Algonquin and Lake Nipissing beaches which have respective ages near 12,000 and 6000 years. Since these lakes were formed at the margin of the Laurentian ice sheet during its retreat, it should not be too surprising that the tilts induced in these constant time horizons by the isostatic adjustment process are rather sensitive to the thickness of the lithosphere. As we will show through discussion of extensive new calculations of deglaciation-induced relative sea level histories, the lithospheric thickness preferred by these strandline tilt data agrees with that found previously on the basis of the analysis

of east coast sea level histories [*Peltier*, 1984*a*, *b*] when allowance is made for the trade-off between this parameter and lower mantle viscosity.

The most important new data set which we will discuss in this paper, however, consists of tide gauge observations of the present-day rates of relative sea level change obtained by extracting the secular rate of sea level change from individual tide gauge records of particularly long duration. The data which we will analyze consist, in part, of the information recently published by the *National Ocean Service* [1983] which comprise time series from roughly 43 tide gauges located along both the east and west coasts of the continental United States. We will also consider the present-day rates of relative lake level change recorded on the large array of gauges distributed throughout the Great Lakes region. If glacial isostatic adjustment were the only ongoing process contributing to present-day relative sea and lake level variations on the North American continent, then the global isostatic adjustment model with parameters fixed by appeal to long time scale ^{14}C-controlled relative sea level histories should accurately predict the present-day rates of vertical motion extracted from the tide gauge data. As we will show, although the relatively rapid rates of present-day lake level fall observed in the Great Lakes region are nicely reconciled by the same isostatic adjustment model which fits long time scale ^{14}C-controlled relative sea level histories, the relatively low rates of present-day sea level rise observed along the east coast of the continental United States across the peripheral bulge produced by the Laurentian ice sheet load are systematicaly higher than those predicted by the isostatic adjustment model. In this region and also along the U.S. west coast, the model is used to filter the tide gauge data and so to reveal more clearly the nature of the component of present-day relative sea level change which is not attributable to glacial isostasy. This observed residual has come to play an important role in recent discussions of climate change [e.g., *Gornitz et al.*, 1982; *Hansen et al.*, 1982] as it has been interpreted as requiring some current retreat of continental ice sheets and/or small glaciers [e.g., *Meiers*, 1984]. If this process is occurring, it could be a first consequence of the amelioration of planetary climate which is expected due to the increasing atmospheric concentrations of CO_2 and other "greenhouse" gases which has accompanied the industrial revolution. There is therefore a great deal of current interest in relative sea level data as a potential indicator of impending climate change [e.g., *Barnett*, 1983]. These analyses will be discussed in section 3 of this paper, and our main conclusions will be reviewed in section 4.

2. Global Model of Glacial Isostatic Adjustment and Relative Sea Level Change

Variations of relative sea level forced by a planetary scale deglaciation event are governed ultimately by complex gravitational interactions between the cryosphere, the aquasphere, and the solid earth. As ice sheets melt and their meltwater enters the ocean basins, the earth deforms in response to the removal of the surface load associated with individual ice sheets and in response to the application of surface load associated with the addition of water to the ocean basins. As the earth deforms its gravitational field is modified by redistribution of matter caused by the deformation. These modifications are in turn felt by the oceans in which meltwater is obliged to distribute itself in such a way as to maintain the ocean surface as an equipotential. Beginning with the paper by *Peltier* [1974], a rather complete model which incorporates the full effects of the gravitational interaction between these three components of the system in determining relative sea level change has been developed over the past decade. This paper showed how one could employ the viscoelastic principle of correspondence [e.g., *Biot*, 1954] to construct the solution for the forced response of a radially stratified viscoelastic sphere to the addition onto its surface of a point mass load. Since both ice sheet disintegration and ocean basin loading by meltwater may be described in terms of a superposition of such loads it is clear that the solution to this impulse response will be the Green's function required to describe the complex gravitational interaction which ultimately determines postglacial variations of relative sea level. This theory was first applied by *Peltier and Andrews* [1976] to calculate approximate histories of relative sea level variation based upon the assumption that the meltwater produced by ice sheet retreat could be assumed to enter the ocean basins uniformly. *Peltier* [1976] showed how these required Green functions could be constructed using a theory of viscoelastic normal modes. *Farrell and Clark* [1976] showed how the formalism could be employed to account for the full effects of the gravitational interaction between water and ice and therefore how one could actually solve for the manner in which the meltwater had to be distributed over the ocean basins in order to keep the surface of the instantaneous ocean an equipotential at all times. The full theory was first applied to compute postglacial variations of relative sea level by *Clark et al.* [1978] and *Peltier et al.* [1978], who demonstrated that a large fraction of the observed global variability in relative sea level in the age range 0–18 kyear B.P. could be explained in terms of this model. Very extensive new computations with this theory have been recently described by *Wu and Peltier* [1983] and a detailed recent review of the results which have been obtained with it will be found in the work by *Peltier* [1982]. Since the accounts of the theory provided in these references are rather complete, the brief review presented here will be constructed so as to focus attention upon the new issues to be addressed in the context of the present paper.

The first phase of the theoretical sea level calculation involves the construction of Green's function for the impulse response of the surface mass load boundary value problem. This requires solution of the usual equations for conservation of momentum and for the gravitational field which, in the quasi-static limit in which inertial forces are negligible, have the respective forms [e.g., *Backus*, 1967]

$$\nabla \cdot \boldsymbol{\sigma} - \nabla (\rho g \mathbf{u} \cdot \mathbf{e}_r) - \rho_0 \nabla \phi_1 - g_0 \rho_1 \mathbf{e}_r = 0 \tag{1a}$$

$$\nabla^2 \phi_1 = 4\pi G \rho_1 \tag{1b}$$

where the density perturbation is obtained from the linearized continuity equation as

$$\rho_1 = -\rho_0 \nabla \cdot \mathbf{u} - \mathbf{u} \cdot (\partial_r \rho_0) \mathbf{e}_r \tag{2}$$

The momentum equation (1*a*) has been linearized with respect to perturbations from a background hydrostatic equilibrium configuration (p_0, ρ_0, ϕ_0) which satisfies

$$\nabla P_0 = -\rho_0 g_0 \mathbf{e}_r \tag{3a}$$

$$\nabla^2 \phi_0 = 4\pi G \rho_0 \tag{3b}$$

and the parameter G in (1*b*) and (3*b*) is Newton's gravitational constant. In equations (1*a*) and (1*b*) the gravitational potential

perturbation ϕ_1 is in general the sum of two parts, ϕ_2 and ϕ_3, which are the potential of the externally applied load and that due to the internal redistribution of mass caused by the load induced deformation, respectively. In (1*a*) the tensor $\boldsymbol{\sigma}$ is the stress tensor which is connected to the strain tensor through a constitutive relation which embodies the rheological equation of state. Since (1*a*) is a linear equation, if the stress-strain relation is also, then (1*a*) may be considered to be expressed in the complex frequency domain of the Laplace transform variable s rather than the time domain, and it is because of this that one may apply the correspondence principle to such advantage in solving linear viscoelastic problems.

As discussed in section 1, much of the analysis of the glacial rebound problem which has been completed to date has been based upon the assumption that the constitutive relation for the mantle could be assumed to be adequately approximated as a linear Maxwell solid for purposes of this analysis. The conventional one-dimensional spring and dashpot analogue of this solid is shown in Figure 1*a*. In the Laplace transform domain the stress strain relation for this solid takes the form

$$\sigma_{kl}\lambda(s)\, e_{kk}\delta_{kl} + 2\mu(s)e_{kl} \tag{4}$$

where e_{kl} is the strain tensor and $\lambda(s)$, $\mu(s)$ are the frequency dependent modulii [*Peltier*, 1974]:

$$\lambda(s) = \frac{\lambda_1 s + \mu_1 K/\nu_1}{s + \mu_1/\nu_1} \tag{5a}$$

$$\mu(s) = \frac{\mu_1 s}{s + \mu_1/\nu_1} \tag{5b}$$

Inspection of the asymptotic properties of the relation (5) shows that in the short time scale limit ($s \to \infty$) the modulii are such that $\lambda(s) \to \lambda_1$ and $\mu(s) \to \mu_1$, where λ_1 and μ_1 are thus the usual Lamé constants of Hookean elasticity. In the long time scale limit ($s \to 0$), on the other hand, inspection of (5) shows that $\lambda(s) \to K$ and $\mu(s) \to \nu_1 s$ so that the solid behaves as a compressible fluid with Newtonian viscosity ν_1. When we fit the glacial isostatic adjustment model to relative sea level data by finding an appropriate radial viscosity stratification $\nu_1(r)$, with λ_1 and μ_1 fixed by short time scale seismic observations, we are therefore implicity assuming that the viscosity ν_1 is the same steady state viscosity which would govern the mantle convection process. In section 1 I pointed to the existence of some new geophysical data which may be taken to imply that at least insofar as the lower mantle is concerned, glacial rebound may not be sensing the steady state value of the creep resistance but rather some lower value associated with a transient anelastic component of the relaxation as first suggested by *Weertman* [1978].

One way in which such a transient component of the rheology can be incorporated into a linear viscoelastic analogue is through use of a simple Burgher's body description of the material constitutive relative between stress and strain. Such a solid was first analyzed in the context of the glacial rebound problem by *Peltier et al.* [1981] and a conventional one-dimensional spring and dashpot representation of it is shown in Figure 2*c*. The Burgher's body solid is really just a superposition of the so-called standard linear solid element shown in Figure 2*b* and the Maxwell analogue shown in Figure 2*a*. It requires two extra parameters to describe it, a second elastic shear modulus μ_2 and a second viscosity ν_2. The frequency dependent modulii analogous to those for the Maxwell solid given in equations (5) for the Burgher's body solid were first derived by *Peltier et al.* [1981] for a three-dimensional material and have more recently been discussed by *Yuen and Peltier* [1982] in connection with elastic gravitational free oscillations and in *Peltier* [1982, 1984*a*, *b*] in connection with the general question of mantle rheology. The frequency dependent modulii which replace (5) for this solid were found to be

$$\lambda(s) = \left\{\lambda_1 s^2 + \left[\left(\frac{\mu_1+\mu_2}{\nu_2} + \frac{\mu_1}{\nu_1}\right)\left(\lambda_1 + \frac{2}{3}\mu_1\right) - \frac{2}{3}\frac{\mu_1\mu_2}{\nu_2}\right]s + \frac{\mu_1\mu_2}{\nu_1\nu_2}\left(\lambda_1 + \frac{2}{3}\mu_1\right)\right\}\left[s^2 + \left(\frac{\mu_1+\mu_2}{\nu_2} + \frac{\mu_1}{\lambda_1}\right) + \frac{\mu_1\mu_2}{\nu_1\nu_2}\right]^{-1} \tag{6a}$$

$$\mu(s) = \frac{\mu_1 s}{s + \mu_1/\nu_1}\left[\frac{(s+\mu_2/\nu_2)(s+\mu_1/\nu_1)}{(s+\mu_2/\nu_2)(s+\mu_1/\nu_1) + \mu_1 s/\nu_2}\right] \tag{6b}$$

One of the main new points which we wish to stress in this paper concerns the connection between the applicability of models like that embodied in (6) to the interpretation of postglacial rebound data and those embodied in (5). Note from (6*b*) that in the long time limit, $s \to 0$ the shear modulus $\mu(s) \to s\,\nu_1$ as before so that the steady state viscosity ν_1 essentially governs the relaxation and this proceeds as would that for a Newtonian viscous fluid with viscosity ν_1. Consider, however, the particular example of the Burgher's body solid embodied in (6) in the limit that the modulus $\mu_2 \ll \mu_1$. As $\mu_2 \to 0$, we note from (6*b*) that

$$\begin{aligned}\lim_{\mu_2 \to 0} \mu(s) &= \frac{\mu_1 s}{s + \mu_1\nu_1}\left[\frac{s(s+\mu_1/\nu_1)}{s(s+\mu_1/\nu_1) + \mu_1 s/\nu_2}\right] \\ &= \frac{\mu_1 s}{s + \mu_1/\nu_1 + \mu_1/\nu_2} \\ &= \frac{\mu_1 s}{s + \mu_1[(\nu_1+\nu_2)/\nu_1\nu_2]} \\ &= \frac{\mu_1 s}{s + \mu_1/\nu_{\text{eff}}}\end{aligned} \tag{7}$$

so that the Burgher's body solid, in the limit that the relaxed shear modulus is close to zero, will behave as a Maxwell solid with "effective" viscosity:

$$\nu_{\text{eff}} = \frac{\nu_1\nu_2}{\nu_1 + \nu_2} \tag{8}$$

If the steady state viscosity ν_1 is such that $\nu_1 \gg \nu_2$, then $\nu_{\text{eff}} \approx \nu_2$ and application of the Maxwell analogue to invert for the viscosity of a region whose rheology is actually of the Burgher's body form described by (6) (such as may be the case for the lower mantle, for example) with a strong transient component of the creep ($\mu_2 \ll \mu_1$) and $\nu_1 \gg \nu_2$ will actually and rather accurately return the value of the transient viscosity ν_2. This fact should be kept clearly in mind in interpreting the analyses to be presented in this paper. Although we will continue to employ the Maxwell solid embodied in the frequency dependent modulii (5) for purposes of analysis, the lower mantle viscosity inferred on the basis of this analysis could very well be a transient value, as originally suggested by *Weertman* [1978]. A more detailed discussion of the application of Burgher's body rheologies, which do not satisfy the above asymptotic conditions, to interpretation of the rebound data will be found in the work by *Peltier et al.* [1985]. A preliminary analysis was presented by *Peltier* [1985*c*].

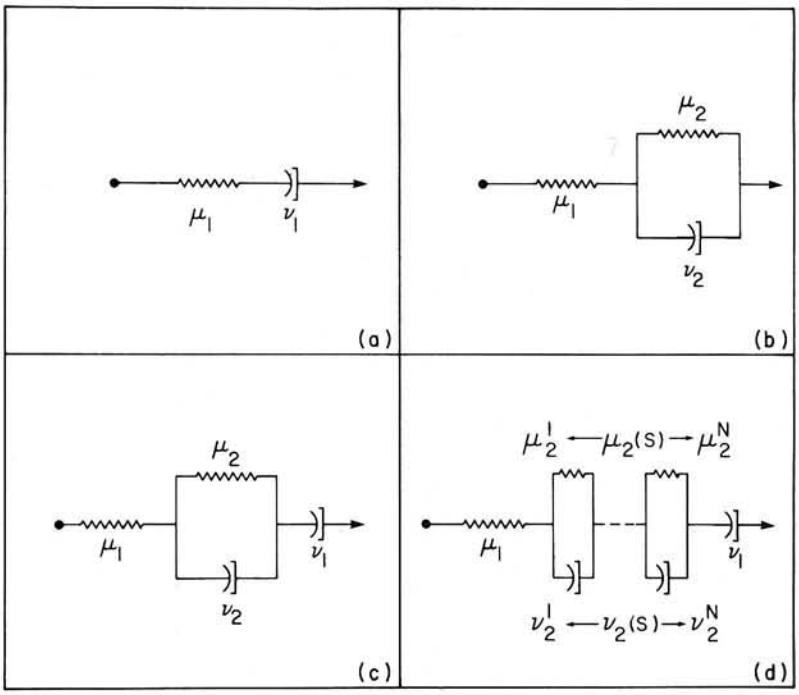

Fig. 2. Conventional one-dimensional spring and dashpot analogues of linear viscoelasticity. (*a*) The Maxwell solid, (*b*) the standard linear solid, (*c*) the Burgher's body solid, and (*d*) a generalized Burgher's body containing a spectrum of Kelvin-Voight elements which characterize the anelasticity and which is required to explain the independence of Q on frequency which is characteristic of the seismic band (e.g., see *Peltier et al.* [1981]).

Given an appropriate rheological equation of state as discussed above, the first phase of the relative sea level calculation is completed by solving equations (1) in the frequency domain to determine the deformation induced by a point mass load placed on the surface of the viscoelastic planet at $t = 0$ and instantaneously removed. Symmetry considerations demand that this response depend only upon r, s, and the angular distance θ between a field point and the point of application of the load. Fundamental solutions are therefore spheroidal and have the following vector harmonic decompositions:

$$\mathbf{u} = \sum_{l=0}^{\infty} \left[U_l(r, s) P_l(\cos\theta)\hat{e}_r + V_l(r, s) \frac{\partial P_l}{\partial \rho}(\cos\theta)\hat{e}_\theta \right] \tag{9a}$$

$$\phi_1 = \sum_{l=0}^{\infty} \phi_l(r, s) P_l(\cos\theta) \tag{9b}$$

$$\nabla \cdot \mathbf{u} = \sum_{l=0}^{\infty} X_l(r, s) P_l(\cos\theta) \tag{9c}$$

Substitution of (9) into (1) reduces the set of original partial differential equations to a simultaneous set of six ordinary differential equations of the form

$$\frac{d\mathbf{Y}}{dr} = \mathbf{A}\mathbf{Y} \tag{10}$$

where the solution six-vector $\mathbf{Y} = (U_l, V_l, T_{rl}, T_{\sigma l}, \phi_l, Q_l)$ and the spectral amplitudes T_{rl}, $T_{\theta l}$, Q_l are related to the amplitudes in the expansions (9) by

$$T_{rl} = \lambda X_l + 2\mu \dot{U}_l \tag{11a}$$

$$T_{\theta l} = \mu(\dot{V}_l - \frac{1}{r} V_l + \frac{1}{r} V_l) \tag{11b}$$

$$Q_l = \dot{\phi}_l + \frac{(l+1)}{r} \phi_l + 4\pi G\rho_0 U_l \tag{11c}$$

The elements of the A matrix of coupling coefficients are listed in equations (3.12) of *Peltier* [1982]. Solutions to (10) are conveniently expressed in terms of the set of dimensionless scalars called Love numbers which are functions of r, s, and l defined through the relations

$$\begin{bmatrix} U_l(r, x) \\ V_l(r, s) \\ \phi_{3l}(r, s) \end{bmatrix} = \phi_{2,l(r)} \begin{bmatrix} h_l(r, s)/g_0 \\ l_l(r, s)/g_0 \\ -k_l(r, s) \end{bmatrix} \tag{12}$$

All of the information on earth structure is embedded in these Love numbers. The normal mode theory first developed by *Peltier* [1976] and recently extended by *Peltier* [1985*a*] shows that each of these impulse response Love numbers has a time domain representation in the form (e.g., for h_l at the surface $r = a$)

$$h_l(a, t) = \sum_j r_j^l e^{-s_j^l t} + h_l^E(a)\delta(t) \tag{13}$$

where the s_j^l are poles of the solution on the real axis of the negative half of the complex s plane and the r_j^l are the residues at these poles. These quantities are now computed using the extension of the original normal mode theory recently provided by *Peltier* [1985*a*, *b*].

Given these Love numbers, the Green's functions required for the glacial isostatic adjustment calculations may be simply computed by substitution into equation (9) and summing the infinite series. For example, the Green's function for radial displacement takes the form

$$u(\theta, t) = \frac{a}{m_e} \sum_{l=0}^{\infty} h_l(a, t) P_l(\cos\theta) \tag{14a}$$

Using the Love numbers, Green's functions may also be computed for other signatures of the response to surface loading. Those for the free air gravity anomaly $\alpha(\theta, t)$ and the pertur-

bation of the gravitational potential $\phi(\theta, t)$ are especially important and take the form [e.g., *Longman*, 1963]

$$\alpha(\theta, t) = \frac{g}{m_e} \sum_{l=0}^{\infty} [1 + 2h_l - (l+1)k_l]P_l(\cos\theta) \qquad (14b)$$

$$\phi(\theta, t) = \frac{ag}{m_e} \sum_{l=0}^{\infty} [1 + k_l - h_l]P_l(\cos\theta) \qquad (14c)$$

The Green's function for the gravitational potential perturbation given in (14*c*) is in fact the main ingredient required to obtain gravitationally self consistent solutions for the relative sea level variations forced by an ice sheet melting event. The "sea level equation" which forms the basis of this calculation is most simply understood by considering a scenario in which all of the ice sheets which were on the surface at glacial maximum melted instantaneously. If $L(\theta, \phi)$ is used to denote the ice thickness removed from position (θ, ϕ) at $t = 0$ and $S(\theta, \phi, t)$ the amount of water added to the ocean at position (θ, ϕ) and time t, then we may compute the change of gravitational potential on the surface by convolution of the surace loads L and S with the Green's function ϕ in (14*c*) to obtain

$$\phi(\theta, \phi, t) = \rho_I \, \phi * L + \rho_w \, \phi * S \qquad (15)$$

where the asterisks indicate convolution over the ice and water, respectively, and where ρ_I and ρ_w are the densities of ice and water, respectively. From (14*a*) it is clear that (15) includes the change of potential due to vertical displacement of the surface of the solid earth (since ϕ contains h_l) as well the contribution due to the internal redistribution of matter in the planetary interior (since ϕ contains k_l). The change in potential (15) will force an adjustment of the local bathymetry in the amount [*Farrell and Clark*, 1976]

$$S = \frac{\phi(\theta, \phi, t)}{g} + C \qquad (16)$$

where C is determined by the requirement of mass conservation. Now (16) is a result of first-order perturbation theory, which is valid for sufficiency small changes of the local bathymetry S. It is clear by construction that S is the local variation of sea level with respect to the deformed surface of the solid earth and is therefore precisely that which is recorded in relative sea level observations. Substituting (16) into (15) results in the equation

$$S = \rho_I \, (\phi/g) * L + \rho_w \, (\phi/g) * S + C \qquad (17)$$

To determine the constant C, we note that the integral of $\rho_w S$ over the surface of the oceans must equal the instantaneous value of the total mass which has been lost by ice sheet disintegration at time t. Therefore

$$C = -\frac{M_I(t)}{\rho_w A_0} - \frac{1}{A_0} \left\langle \rho_I \frac{\phi}{g} * L + \rho_w \frac{\phi}{g} * S \right\rangle_0 \qquad (18)$$

where $\langle \ \rangle_0$ indicates integration over the oceans which are assumed to have total area A_0 and where $M_I(t)$ is the mass loss history of the ice sheets and the ratio $M_I(t)/\rho_w \cdot A_0$ the so-called eustatic water rise. Given a model of the internal viscoelastic stratification of the planet embodied in the Green's function ϕ and a model of the deglaciation history embodied in a function $L(\theta, \phi, t)$, the integral equation (17) may be inverted to obtain $S(\theta, \phi, t)$ and therefore to predict the relative sea level history which should be observed at any point on the surface where water meets land. The numerical methods which have been developed to solve the sea level equation (17) have been discussed in detail by *Peltier et al.* [1978] and more recently by *Wu and Peltier* [1983]. This realistic and gravitationally self-consistent model will be employed for all of the calculations to be discussed in the present paper. Furthermore, all calculations will be based upon the deglaciation history ICE-2 which has recently been tabulated by *Wu and Peltier* [1983]. The new calculations discussed in the following sections will therefore focus upon the ability of vertical motion observations to constrain the parameters governing the radial viscoelastic structure of the planet.

3. RADIAL VISCOELASTIC STRUCTURE AND DEGLACIATION-INDUCED VERTICAL MOTION

In the calculations to be discussed here we will employ a range of different viscoelastic parameterizations of the radial earth structure. Although these will all be based upon the use of a Maxwell analogue, it should be kept clearly in mind that the lower mantle viscosity inferred on the basis of fitting these models to the vertical motion data could very well represent a transient component of the viscosity spectrum rather than the steady state value. As mentioned in the introduction, it is becoming increasing clear that this may be the case. The models which we employ will therefore differ from one another only in the elastic components of the structure which are determined by the two Lamé parameters $\lambda(r)$ and $\mu(r)$ and the density field $\rho(r)$. Although these components of the structure are rather well constrained by seismic body wave and free oscillation observations, it should be clear that if the observed seismic structures are simply inserted into the field equations (1), then certain physical processes will be induced in the viscous regime which may or may not, in fact, be operative. For example, the second term on the left-hand side of equation (1) describes the extra body force which the viscoelastic material feels by virtue of the fact that the medium which is caused to deform by the surface ice and water loads is subject to a hydrostatic prestress. This extra body force will be particularly strong near an interface across which the density is discontinuous. In all realistic elastic models of earth structure such as PREM or 1066B such discontinuities of density (or near discontinuities) are found at both 420 km and 670 km depth which correspond to the depths of occurrence of the olivine-spinel and spinel-periclase phase transformations. When these internal boundaries are deflected by external surface loads, they will therefore induce a buoyant restoring force due to the presence of the second term on the left-hand side of (1). It is somewhat debatable, however, whether such a buoyant restoring force could be produced by equilibrium phase transformations since one might expect that as the boundaries were distorted by the applied surface loads, material would simply change phase so as to keep the boundary on the equilibrium Clapeyron curve. As recently discussed by *Peltier* [1985*a*, *b*], however, to the extent that the phase boundaries may be approximated as univariant transitions the time scale required for the material to change phase is the thermal diffusion time scale which is long compared to the loading time scale, and therefore adiabatic phase boundaries could behave as nonadiabatic chemical boundaries insofar as their response to short time scale surfaces loading is concerned. In the past several years we have shown that the observed free air gravity anomalies over Canada and Fennoscandia may require these phase boundaries to behave in just this way [*Peltier and Wu*, 1982; *Wu and Peltier*, 1983; *Peltier*, 1985*a*, *b*]; otherwise, it has proven impossible to fit the free air gravity anomalies with

TABLE 1. Elastic Models Employed in the Vertical Motion Calculations

Model	Quantity	0–420 km	Δ	420–671 km	Δ	671–2886 km	Δ	Core
1066B	density (kg m^{-3})	varies	141	varies	272	varies	111	varies
CML64	density (kg m^{-3})	3959	141	4100	272	4372	4414	p (1066B)-1191
	P velocity (m s^{-1})	9323		9945		11013		v_p (1066B)-2657
	S velocity (m s^{-1})	5219		5475		6117		v_s (1066B)
CML64D	density (kg m^{-3})	4321	141	4462	272	4734	4414	p (1066B)-829
	P velocity (m s^{-1})	as CML64						
	S velocity (m s^{-1})	as CML64						
CML64E	density (kg m^{-3})	as CML64D						
	P velocity (m s^{-1})	8317		9730		12341		v_p (1066B)
	S velocity (m s^{-1})	4550		5260		6680		v_s (1066B)
CML64F	density (kg m^{-3})	4011	282	4293	544	4837	4414	p (1066B)-726
	P velocity (m s^{-1})	as CML64E						
	S velocity (m s^{-1})	as CML64E						
CML64G	density (kg m^{-3})	3436	493	3929	952	4881	5094	p (1066B)-2
	P velocity (m s^{-1})	as CML64E						
	S velocity (m s^{-1})	as CML64E						
CML64H	density (kg m^{-3})	3966.5	282	4248.5	544	4792.5	4686	p (1066B)-498.5
	P velocity (m s^{-1})	as CML64E						
	S velocity (m s^{-1})	as CML64E						
CML64I	density (kg m^{-3})	4010	247	4257	476	4733	4890	p (1066B)-354
	P velocity (m s^{-1})	as CML64E						
	S velocity (m s^{-1})	as CML64E						

Earth mass for CML64 is 0.934 × mass(1066B), same as 1066B for other models. Some models run with whole earth compressible, others with only compressible lithosphere.

the same Maxwell analogue of the internal viscoelastic stratification as that which is required by the relative sea level data. *Peltier* [1985*c*] and *Peltier et al.* [1986] discuss the extent to which the internal buoyancy which these data apparently require may be eliminated by substituting a more complicated representation of the rheology of the mantle such as that embodied within the Burgher's body whose frequency dependent modulii are given in equations (6). It could prove to be possible to reduce the amount of buoyancy required by the free air gravity data by introducing this extra rheological complexity, a fact which is clearly important to the understanding of long time scale mantle dynamics [*Peltier*, 1985*a*, *b*].

The models to be employed in the calculations to be discussed below include two characteristically different types. Most are members of a set of models labeled CML64A-G which consist of simple homogeneous multiple layer approximations to the seismically realistic model 1066B. These models each include a compressible surface lithosphere with variable thickness, an upper mantle with constant properties from the base of the lithosphere to a depth of 420 km, a transition region bounded by variable strength discontinuities of elastic properties at 420 and 670 km depth, a lower mantle with constant elastic properties extending from a depth of 670 km to the core-mantle boundary, and an inviscid core with elastic structure the same as that in model 1066B. The second model type whose response characteristics we will discuss consists of the seismically realistic model 1066B itself. A list of the properties of models CML64A-G is provided in Table 1. Those for model 1066B are identical to the properties listed by *Gilbert and Dziewonski* [1975]. The sequence of models in the set CML64 becomes increasing like 1066B as A → G. For example, the members C, D comprise models which are incompressible from the base of the lithosphere to the core mantle boundary, whereas models F and G are everywhere compressible. Note also that models F and G differ in the strengths of the discontinuities which bound the transition region, the former having magnitudes similar to those in 1066B, whereas the latter have magnitudes equal to those delivered by a model whose three mantle layers have the same average properties as 1066B. The discontinuities in the latter model are clearly much stronger than those in the former and therefore the internal buoyancy induced in this model when its internal boundaries are deflected will be in excess of that delivered by the weak discontinuity analogue which is otherwise identical. As we will document in what follows, there are nonnegligible trade-offs between the viscous component of the structure inferred by fitting such models to vertical motion observations and the elastic "basic state" upon which this viscous structure is superimposed. We will proceed to address this issue below.

3.1. *Relative Sea Level Histories and the Trade-off Between Lower Mantle Viscosity and Lithospheric Thickness*

Although relatively few extensive studies of the application of the gravitationally self-consistent sea level equation (18) to the understanding of viscoelastic earth structure have appeared, those which have demonstrate clearly the potential which the model has to contribute usefully to the resolution of this important geodynamic problem. The initial integrations discussed by *Clark et al.* [1978] were based upon Green's functions for a model with 1066B elastic structure, a uniform mantle viscosity of 10^{21} Pa s, and no lithosphere. *Wu and Peltier* [1983] added a lithosphere to the model, of conventional thickness 120.7 km, and investigated the sensitivity of RSL predictions to the variation of lower mantle viscosity. These analyses, which were all based upon a Maxwell parameterization of the internal viscoelasticity, demonstrated that in terms of this analogue the lower mantle viscosity could not be substantially higher than that in the upper mantle (which is well constrained to a value near 10^{21} Pa s), although some of the RSL data near the center of rebound preferred some increase of viscosity to a lower mantle value near 3×10^{21} Pa s. Although the model fits to the relative sea level (RSL) observations at sites inside the ice margins were rather good, at exterior sites such as those along the U.S. east coast to the

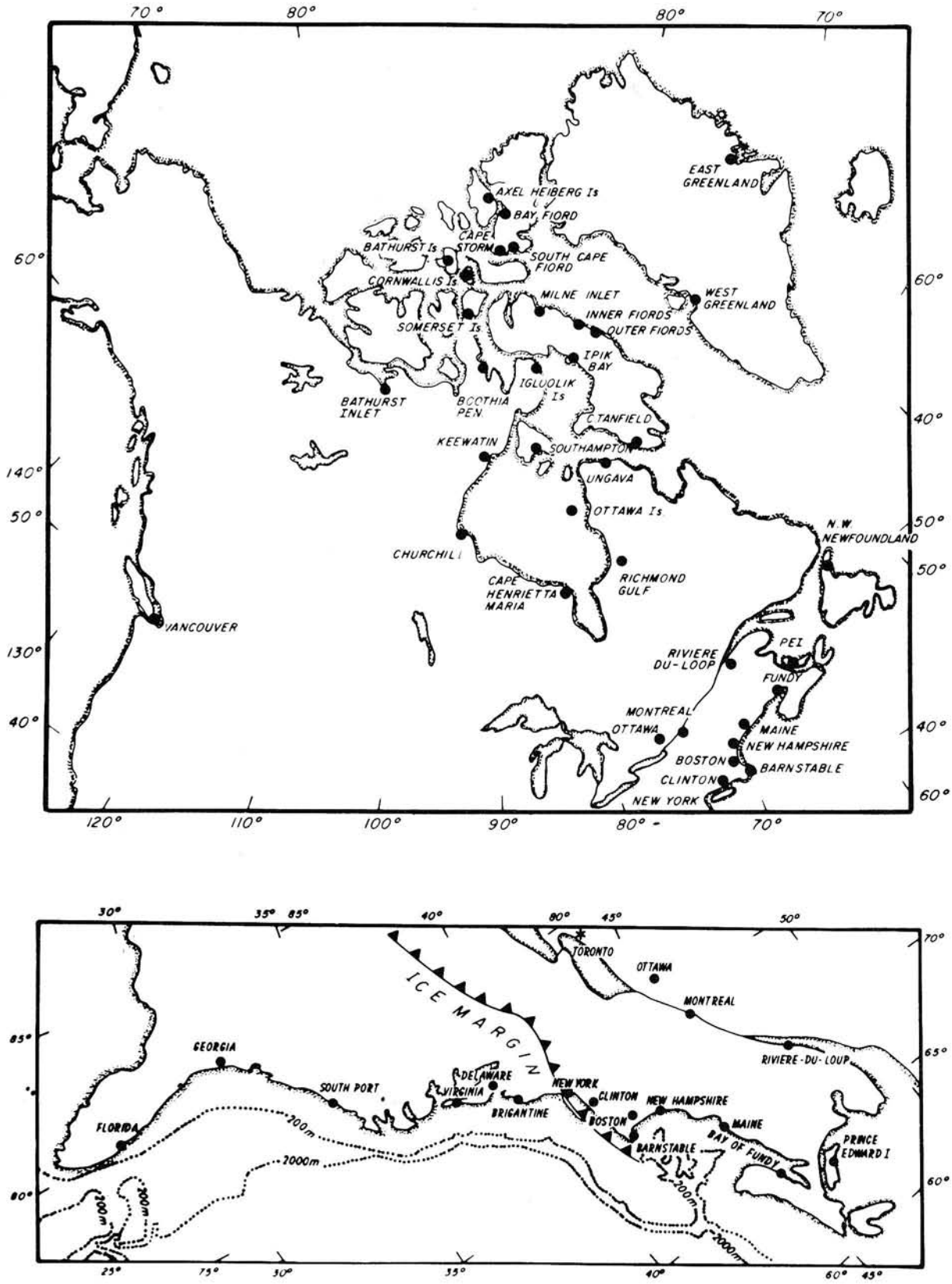

Fig. 3. Location map for North America sites for which ^{14}C-controlled RSL histories are available.

south of the ice margin the fits were extremely poor. *Peltier* [1984*a*, *b*] showed that the error between the predicted RSL curves at exterior sites and those observed varied systematically along the coast and that the misfits could be reduced to zero at almost all sites by simply increasing the thickness of the lithosphere to a value somewhat in excess of 200 km. In fact, a thickness near 245 km appeared to be required when the viscosity of the deep mantle was fixed to a value equal to that in the upper mantle of 10^{21} Pa s. It was pointed out by *Peltier* [1984*a*, *b*], however, that there was a trade-off between

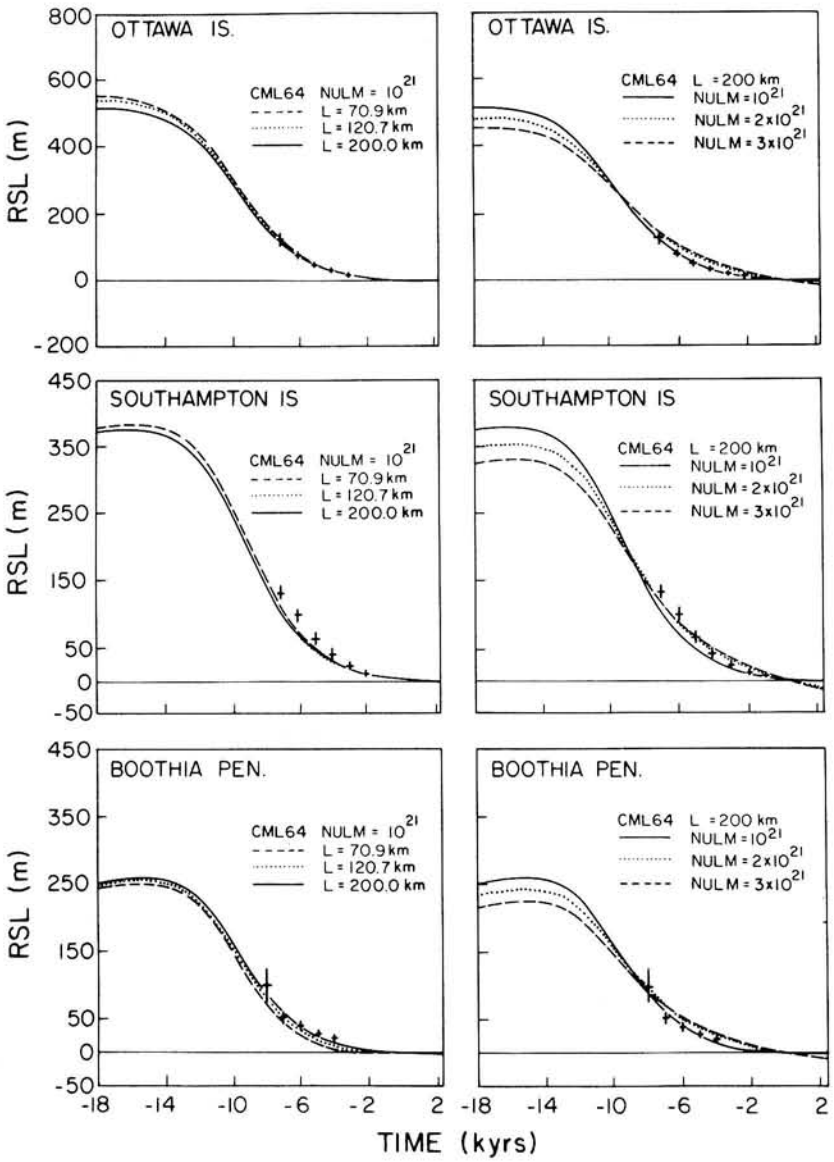

Fig. 4. Comparisons between observed and predicted RSL curves at three of the sites shown on the location map of Figure 3. The site names on the individual plates correspond to those on the map. These figures illustrate the sensitivity of RSL predictions at these sites to variations of lower mantle viscosity and lithospheric thickness. The theoretical calculations employ elastic structure CLM64.

lithospheric thickness and lower mantle viscosity such that increases of the latter had to be compensated by decreases of the former. No systematic investigation of this trade-off was presented there, however, and this important point will be the first to be discussed in the present section.

The extensive sequence of comparisons shown in Figures 4–9 are for relative sea level observations at sites on the North American continent shown on Figure 3, and all calculations in this sequence employ the simple elastic structure CML64. The separate plates on each figure are arranged in pairs, one pair for each of the 18 sites for which the comparison between theory and observation is shown. The first member of each pair illustrates the sensitivity of the predictions at each site to variations of lithospheric thickness with ν_{LM} (the lower mantle viscosity NULM on Figures 4–9) fixed at a value of 10^{21} Pa s for values of lithospheric thickness $L = 70.9$ km, 120.7 km, and 200.0 km. The upper mantle viscosity is maintained at 10^{21} Pa s. The second member of each pair of plates illustrates the sensitivity of the predictions to variations of ν_{LM} with L fixed at 200 km. Figure 4 shows the results of these sensitivity tests for three sites which are within the 18 kyear B.P. ice margin, Ottawa Islands, Southampton Island, and the Boothia Peninsula. Figure 3 shows precise geographic locations of these sites. Inspection of these new comparisons at representative interior sites demonstrates that the response at such locations is only very weakly dependent upon lithospheric thickness but rather sensitive even to relatively small changes of the viscosity of the deep mantle. Some sites, such as the Ottawa Islands, strongly prefer the uniform viscosity model, whereas others like Southampton Island show somewhat higher present-day emergence rates and thus prefer models with a slightly elevated lower mantle viscosity of say 2×10^{21} Pa s when the upper mantle value is held at 10^{21} Pa s. Figure 5 shows similar comparisons for three more sites which were within the ice margin but somewhat closer to the edge than those discussed previously. The locations of these sites, Riviere du Loup, Montreal, and Ottawa are again shown on Figure 3. Although the situation at these locations is similar to that

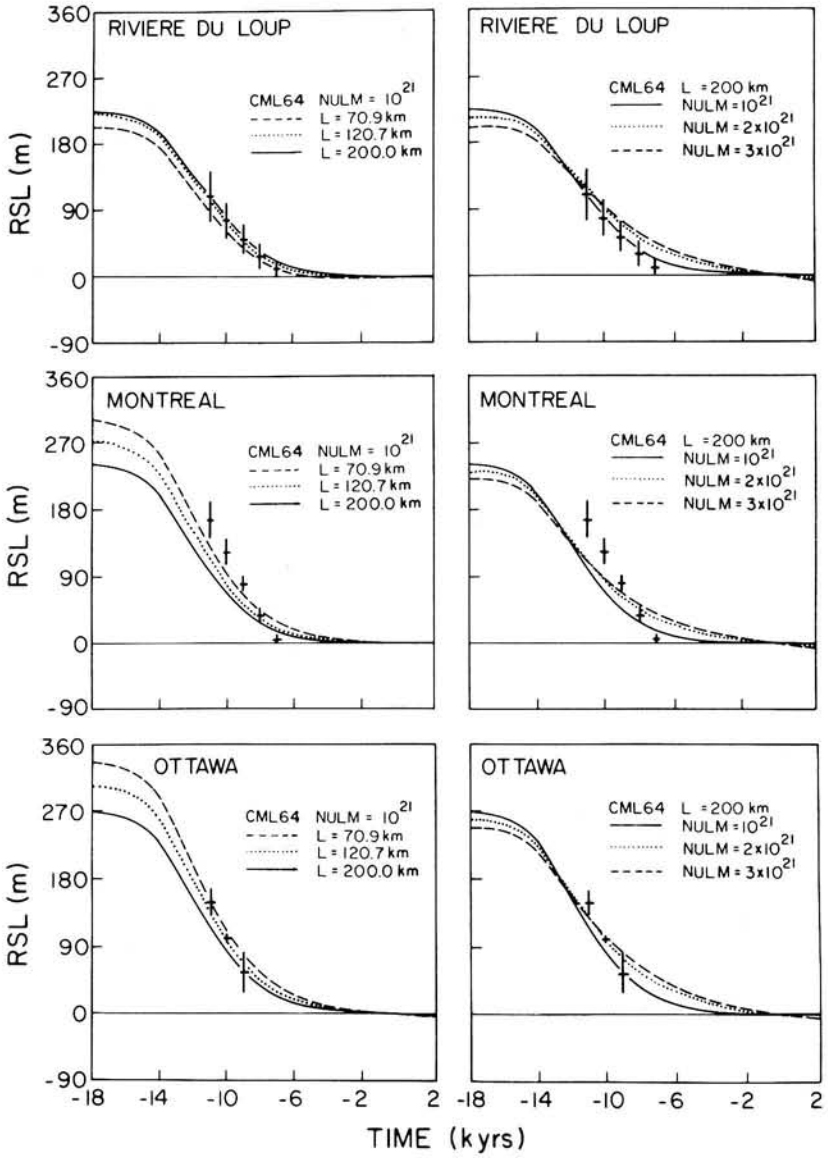

Fig. 5. Same as Figure 4 but for three additional sites.

which obtained at the first three "deep interior" sites, there is a substantial increase of the sensitivity to lithospheric thickness changes. The remaining four figures (Figures 6–9) show similar comparisons for 12 sites located from the 18 kyear B.P. ice margin itself (Maine, New Hampshire, Boston; Figure 6) extending toward the south along the U.S. east coast including Barnstable, Hudson River, Clinton (Figure 7); New York City, Brigantine, Delaware (Figure 8); and Virginia, Southport (North Carolina), and Florida (Figure 9).

From the point of view of the new ideas to be developed in the present paper these U.S. east coast data are especially important. Careful inspection of these comparisons demonstrates that both the northernmost and southernmost sites in this collection (but particularly the southernmost of Southport and Florida) are very much more sensitive to variations in lower mantle viscosity than they are to variations of lithospheric thickness. At the northernmost locations, increasing the viscosity of the lower mantle even by a factor of 3 essentially eliminates the nonmonotonic signature of the predicted relative sea level variation. Since all of the observed relative sea level curves from sites close to the ice margin have this nonmonotonic behavior, with initial emergence followed by later submergence which continues today, it is clear that the viscosity of the lower mantle cannot be even a factor of 3 higher than the viscosity of the upper mantle in the context of the Maxwell parameterization of the radial viscoelastic structure and elastic model CML64. At the southernmost locations of Southport, North Carolina, and Florida (the everglades region), similar sensitivity obtains. However, at Florida the uniform mantle viscosity model is rejected by the observations, since it predicts raised beaches at present in this region where none are observed. As is evident by inspection of the sensitivity calculations, however, increasing the lower mantle viscosity by a factor of 2 brings the predictions into very close accord with the observations. Both of these sensitivities of the RSL predictions at northernmost and southernmost sites along the U.S. east coast are consequences of the effect of lower mantle viscosity variations upon the glacial forebulge which is created by the outflow of material from under the ice sheet in the course of its isostatic compensation. When the ice

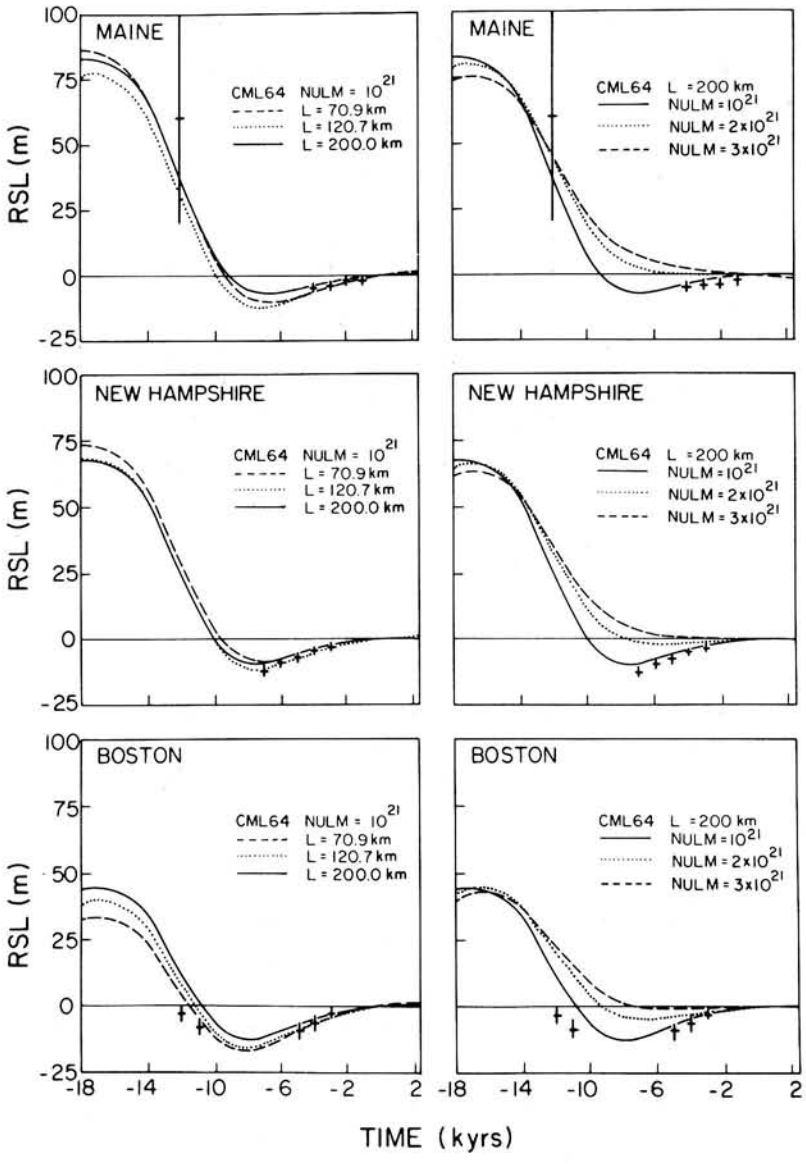

Fig. 6. Same as Figure 4 but for three additional sites.

sheet melts, the system is returned to isostatic equilibrium by the inflow of material from the peripheral region. This inflow causes the collapse of the forebulge which explains the strong submergence of the land relative to the sea in the regions immediately surrounding the ice sheet. Increasing the viscosity of the lower mantle by too large a factor prevents the inward migration of the forebulge as it collapses and therefore eliminates the nonmonotonic variations of RSL which are a characteristic feature of the observations near the ice margin as discussed by *Peltier* [1974]. However, increasing the viscosity of the lower mantle even by a very small factor of 2 increases the width of the forebulge and therefore eliminates the undesirable prediction of raised beaches on the southern flank of the bulge at sites such the Florida location. In the context of our simple parameterization of the viscoelastic structure, then, the viscosity of the lower mantle must be about $\times 2$ the viscosity of 10^{21} Pa s which has been assumed for the upper mantle. This is in accord with the requirement noted above of some RSL data from sites within the ice margin (e.g., the Southampton Island location of Figure 4). It is important for present purposes to note that this inference concerning lower mantle viscosity has been based upon data from sites at which the response is not strongly dependent on lithospheric thickness.

The sensitivity analyses shown on Figures 7 and 8, on the other hand, are for sites which span the crest of the glacial forebulge where lithospheric flexure is most extreme and the RSL predictions at these sites are therefore extremely sensitive to variations of lithospheric thickness L. With the lower mantle viscosity fixed to the same value as the upper mantle viscosity, 10^{21} Pa s, the data from this region clearly prefer the highest value of lithospheric thickness for which explicit calculations have been performed, namely, the value of 200 km. When the lithospheric thickness is smaller than this, too much submergence is predicted over the time interval 0–7 kyear B.P. spanned by the observations. This reinforces the results obtained by *Peltier* [1984*a*, *b*]. It is quite clear by inspection of the results shown on Figures 7 and 8, however, that increasing the viscosity of the lower mantle by the factor which seems to be required to fit the Florida submergence data would require

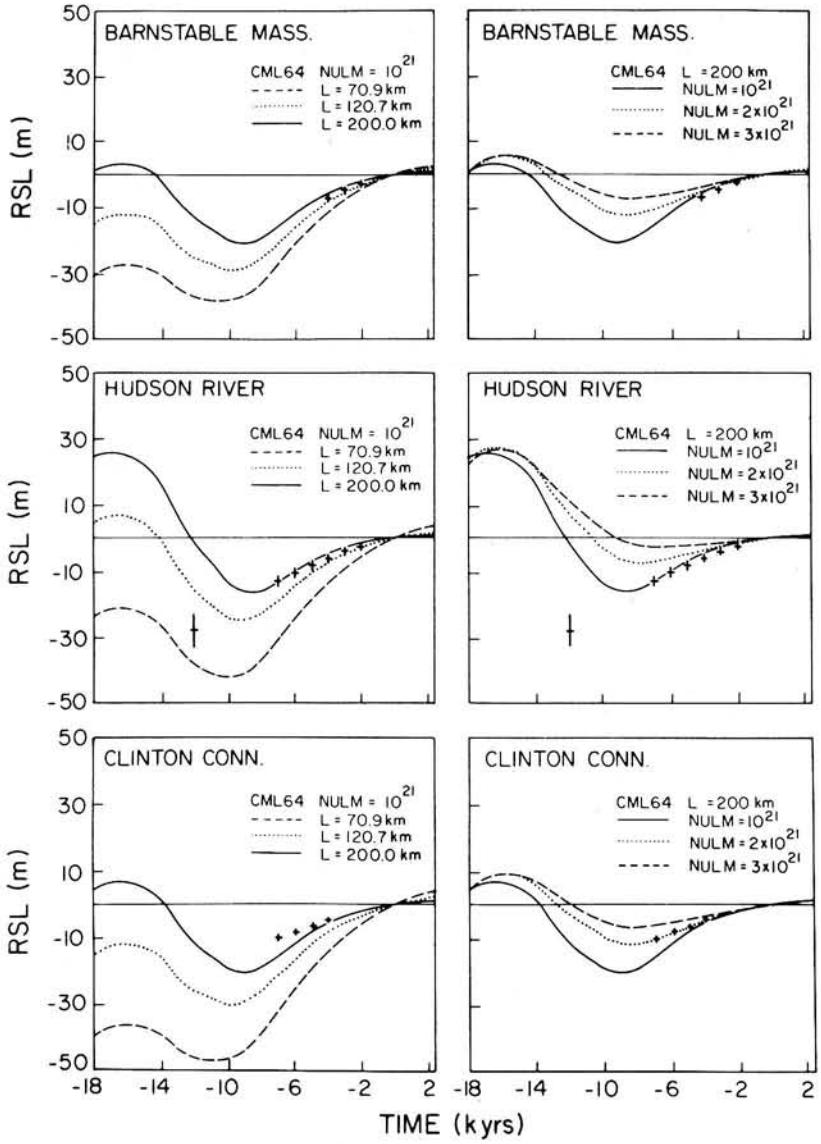

Fig. 7. Same as Figure 4 but for three additional sites.

the lithospheric thickness to be somewhat reduced since increases of both parameters cause the submergence to be diminished in the vicinity of the forebulge crest.

In Figures 10 and 11 this trade-off is investigated in the context of calculations based upon the 1066B parameterization of the radial elastic structure. For purposes of these calculations the lower mantle viscosity was fixed at the value of 2×10^{21} Pa s required by the Florida data and by RSL information from some interior sites. This requirement is not sensitive to the elastic structure employed in the calculations as the model with 1066B elastic structure also predicts raised beaches in Florida when the mantle viscosity is uniform but fits the observations at this site when the lower mantle viscosity is elevated to the value of 2×10^{21} Pa s. The comparisons for the interior sites at Churchill, Ottawa Islands, and Southampton Island on Figure 10, and all others, are shown for lithospheric thicknesses of 120.7 km, 196.6 km, and 245.4 km and establish again that the response at such interior locations is insensitive to lithospheric thickness. The results for New York City, Brigantine, and Delaware, also shown on Figure 10, again demonstrate that a lithospheric thickness near 200 km is required to reconcile the observations when the lower mantle viscosity is 2×10^{21} Pa s. It is important to note that this result, which is reinforced by the comparisons shown on Figure 11 for six more sites along the U.S. east coast, differs somewhat from that obtained previously in this paper in the context of elastic structure CML64, and for 1066B with uniform 10^{21} Pa s lower mantle viscosity obtained by *Peltier* [1984*a*, *b*]. In the latter case a lithospheric thickness of 245.6 km was required to fit east coast RSL data. The somewhat reduced value which is found acceptable here at some sites is a consequence of the slight increase of lower mantle viscosity which has been shown to be required to fit the submergence curve for Florida. Comparison of these results with those obtained for model CML 64 (see Figures 4–9) demonstrates the manner in which the underlying elastic structure contributes to the trade-off between lithospheric thickness and lower mantle viscosity. At all sites, but most importantly at sites in the peripheral bulge region, the deformation associated with elastic model 1066B exceeds that delivered by the simple multiple homogeneous layer parameterization CML64. Therefore the lithospheric thickness re-

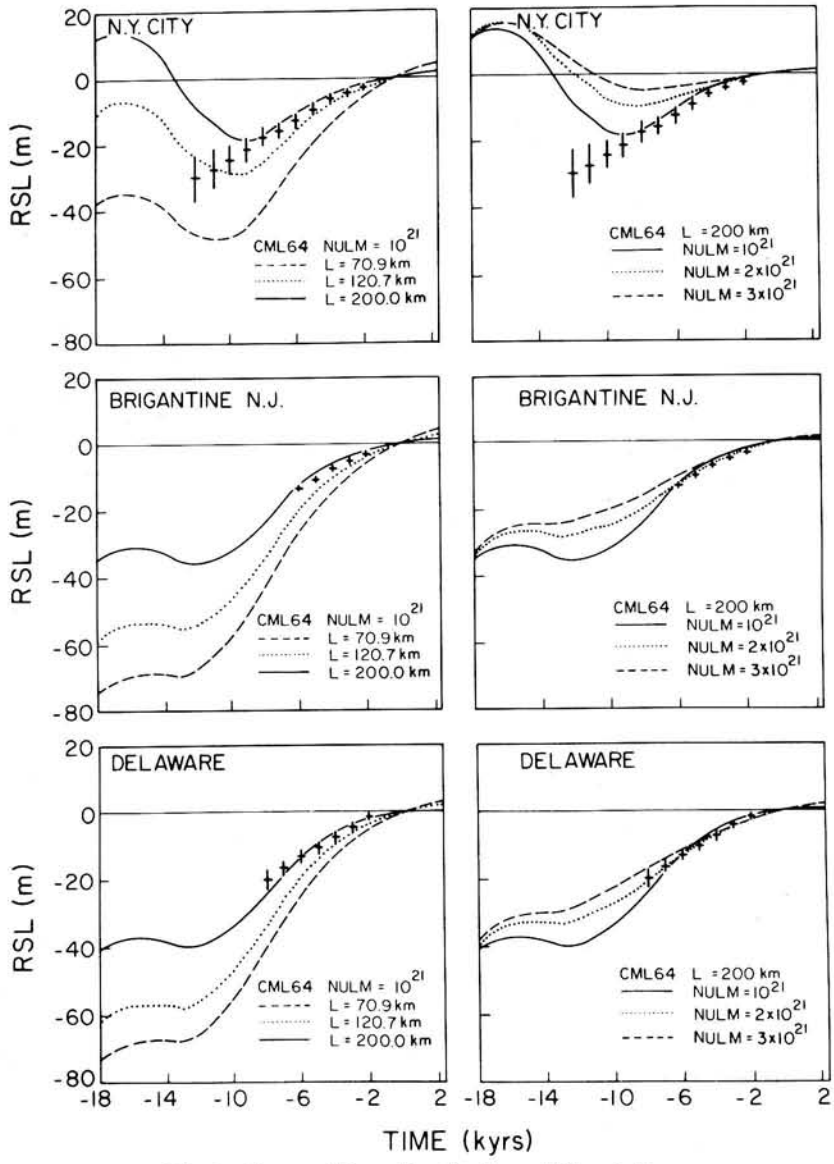

Fig. 8. Same as Figure 4 but for three additional sites.

quired in elastic model 1066B in order to fit peripheral submergence data is greater than that required in model CML64 when the mantle viscosity profiles are identical. There are two major contributing features to this difference. The first is associated with the nonzero compressibility of model 1066B throughout the mantle as opposed to model CML64 which is compressible only in the lithosphere. The second contribution to these differences concerns the more realistic density structure of 1066B and to the enhanced internal buoyancy in 1066B due to the fact that the entire radial density structure is treated as though it were nonadiabatic. The smaller the internal buoyancy which the model contains the thinner, therefore, will be the lithosphere required to reconcile peripheral submergence data. Although substantial internal buoyancy does appear to be required to reconcile observed free air gravity anomalies over the centers of postglacial emergence, it could conceivably prove possible, as mentioned above, to avoid this requirement by invoking the level of rheological complexity embodied in the Burgher's body with finite μ_2. This point is the focus of the discussion by *Peltier* [1985*c*] and *Peltier et al.* [1986].

3.2. *Tide Gauge Constraints on the Present-Day Rate of Eustatic Water Rise in Global Ocean*

Given, as established above, that it is possible to construct simple models of the radial viscoelastic structure of the planet capable of reconciling much of the long time scale variability observed in ^{14}C-controlled records of relative sea level change, it should be clear that we are in a position to employ the models to useful effect in the analysis of other types of data. In this subsection we will address the question as to whether the present-day rates of RSL change revealed on long time series of relative sea level recorded on tide gauges are in agreement with those predicted by the same glacial isostatic adjustment models which fit the ^{14}C record. This issue is a rather important one since several recent articles have appeared which suggest that eustatic sea level is currently rising and that this eustatic rise should be interpreted as "advance warning" of the impending climatic amelioration which is expected as a consequence of the increasing atmospheric loads of CO_2 and other greenhouse gases [e.g., *Hansen et al.*, 1981; *Gornitz et al.*, 1982; *Barnett*, 1983]. These arguments have all been predica-

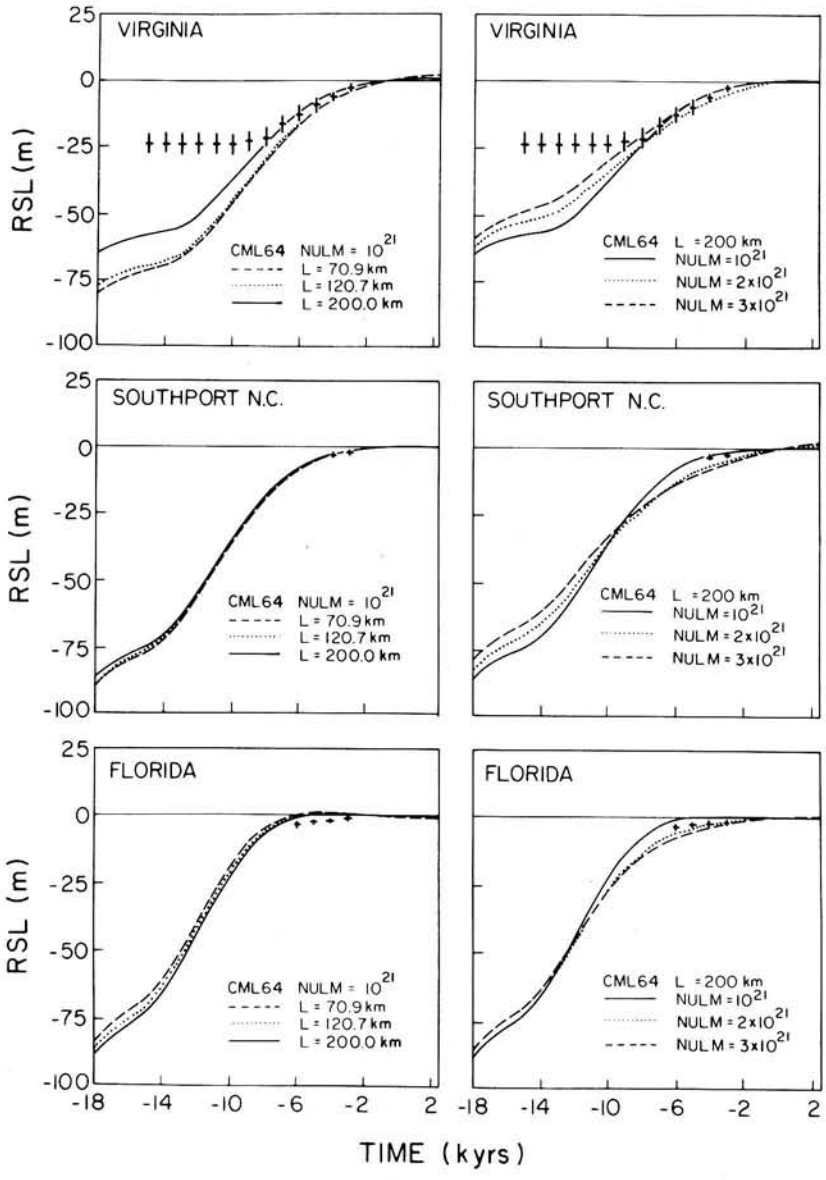

Fig. 9. Same as Figure 4 but for three additional sites.

ted on the assumption that fairly raw tide gauge observed rates of RSL change could be directly employed to infer the present-day eustatic variation of sea level. There are many problems with this, some of which are discussed by *Barnett* [1983], but of perhaps greatest concern among these are those due to the very poor global coverage of the oceans which is provided by the existing tide gauge network and with the fact that observed rates of RSL change may have contributions to them from processes other than eustatic sea level variations. The latter is particularly true of a region like the east coast of the continental United States which as we have seen above, is presently submerging due not necessarily to eustatic increases of sea level but rather to the sinking of the earth which accompanies the flow of material from the peripheral region of initial load uplift toward the central glaciated region in which the land was depressed under the weight of the ice. If RSL data from this peripheral region were directly interpreted as implying a eustatic water rise, it is clear that very substantial error might thereby be made. What we will proceed to do here is to use the isostatic adjustment model to predict the present day rate of RSL rise/fall which should be observed anywhere on the North American and European continents as a consequence of the glacial isostatic adjustment process. We will then use these predications to filter from the secular rate of RSL change observed on all North American tide gauges that part of this signal which is glacial isostatic in origin. As we will see, the residual signal which remains has an interesting and suggestive structure and the isostatic adjustment contribution to the observed signals may be very large.

We will begin by describing the continental scale form of the present-day RSL signal which is predicted by viscoelastic earth models which fit the ^{14}C-controlled sea level histories discussed previously. The best fitting model of those which have been investigated is elastic model 1066B coupled with a lithosphere of thickness 196.6 km, an upper mantle viscosity of 10^{21} Pa s, and a lower mantle viscosity of 2×10^{21} Pa s. Figure 12 shows continent scale maps of the predicted present-day rate of RSL variation (in millimeters per year) for both North America (Figure 12*a*) and Europe (Figure 12*b*), both based upon this model with 1066B elastic structure. Most obvious on each plate is the region of relatively intense present-day sea level fall throughout those areas of each conti-

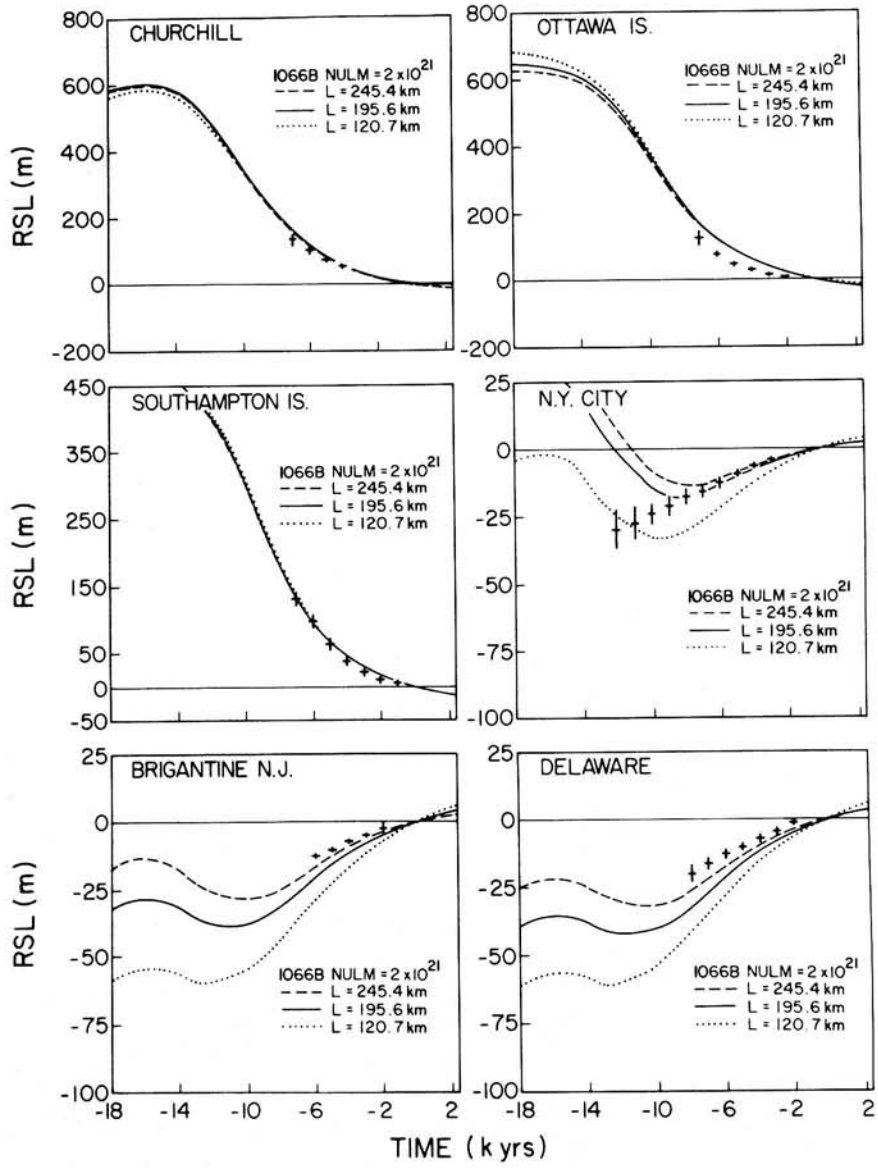

Fig. 10. Comparisons of RSL observations with theoretical predictions as a function of lithospheric thickness based upon the model with 1066B elastic structure at six North American sites.

nent which were actually covered by ice at Würm-Wisconsin maximum 18,000 years ago. Over Hudson Bay, which was under the center of the huge Laurentian ice mass the model predicts present-day land emergence (sea level fall) rates as high as 1.15 cm yr^{-1}. Over the Gulf of Bothnia the model predicts a maximum present-day rate of uplift relative to the geoid of about 0.9 cm yr^{-1}, comparable to but somewhat smaller than the deglaciation-induced vertical motion characteristic of the Hudson Bay region. Of particular interest to us here, however, is the existence and form of the peripheral region of land subsidence which generally surrounds these two central regions of present-day uplift. Inspection of the two vertical motion maps on Figure 12 shows that these peripheral rings of land submergence (sea level rise) are strongly variable in intensity depending upon location around the circumference of the ice-covered regions. For example, in the case of North America the present-day maximum rate of sea level fall along the U.S. west coast is less than 1 mm yr^{-1}, whereas that on the U.S. east coast reaches 2 mm yr^{-1}. The main reason for this disparity between the maximum rates on the two coasts of the United States is that the west coast is much farther from the main Laurentide ice dome and much more strongly influence by the melting of the Cordilleran ice sheet which existed west of the Rocky Mountains and melted earlier than the main Laurentian ice sheet [e.g., *Peltier and Andrews*, 1976]. The greatest rate of present-day submergence in the North American region is, however, to the southeast of Baffin Island where the bulge generated by Laurentian loading interferes constructively with that generated by Greenland loading to force a present-day rate of land submergence with respect to the geoid in excess of 3.2 mm yr^{-1}. A somewhat lower rate (of about 3 mm yr^{-1}) is in fact also predicted for the North American continental interior. It is important to understand the meaning of the rates assigned to such continental interior points where no sea surface exists, with respect to which RSL change may be recorded. They are to be interpreted as the rates which would be measured at these points if a narrow canal were cut from the coast to the point in question and a tide gauge installed there.

The European vertical motion map shown on Figure 12*b*

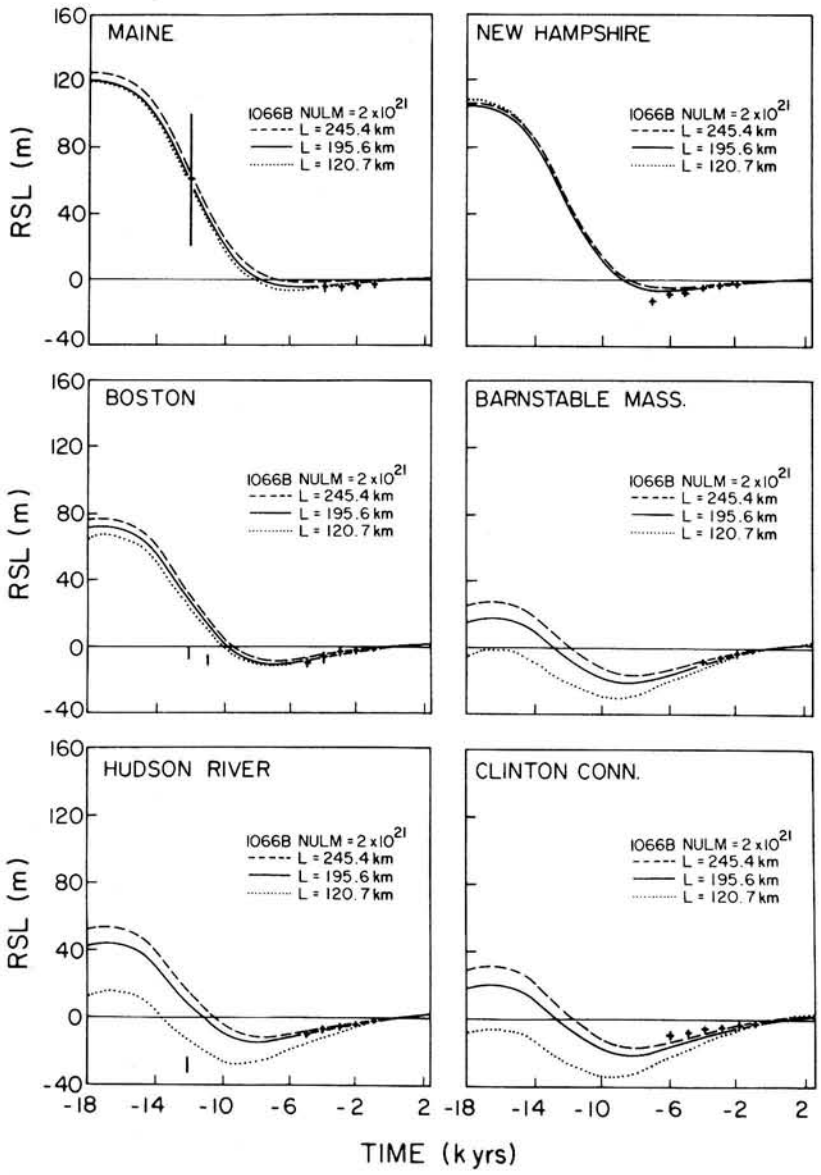

Fig. 11. Same as Figure 10 but for six additional sites.

also displays strong asymmetry of the rates of vertical motion which obtain in the ring-shaped region of peripheral bulge collapse. The most striking property of this region in Europe is that the predicted rates of land submergence along the coast of France are extremely low relative to those which obtain along the U.S. east coast. This is clearly due to the fact that the ice load which existed on Great Britain sat squarely on what would otherwise be the peripheral bulge of the Fennoscandian ice sheet. This ice load is sufficiently large (in the ICE-2 unloading history of *Wu and Peltier* [1983]) to eliminate the submergence which would in its absence be forced by the melting of the Fennoscandian ice dome and slow present-day emergence is in fact predicted by the model throughout most of the British Isles. In Europe the greatest rate of present-day submergence is predicted for islands in the ocean to the immediate northwest of Norway where present-day rates induced by glacial isostatic adjustment approach 2.4 mm yr^{-1}.

Because of the magnitude of these submergence rates associated with glacial isostatic adjustment it is quite clear that they should be easily observable on tide gauge records of even moderate temporal duration. In the present paper I will focus upon the comparison of these predicted rates with tide gauge observed rates at locations along the east and west coasts of North America which are both rather heavily instrumented with gauges whose records may be as long as 100 years in time. In 100 years at the rate of 1 mm yr^{-1} the equilibrium level of the sea will be displaced by an amount of 10 cm, which is a secular change easily observable in monthly averaged data of RSL change. The data set which will be employed to make these comparisons is that recently made available by the *National Ocean Service* [1983], which has compiled secular trend data for all U.S. tide gauges along with standard errors associated with them. These data are shown in Table 2 for both the U.S. east coast gauges (Table 2*a*) and west coast gauges (Table 2*b*). Even a cursory inspection of the numbers in Tables 2*a* and 2*b* shows that these two coasts differ substantially in the nature of the secular trends which have been recorded on tide gauges placed along them. Along the U.S. east coast the observed submergence rates (labeled T) are uniformly positive, indicating rising relative sea level, whereas along the U.S. west coast the rates are highly vari-

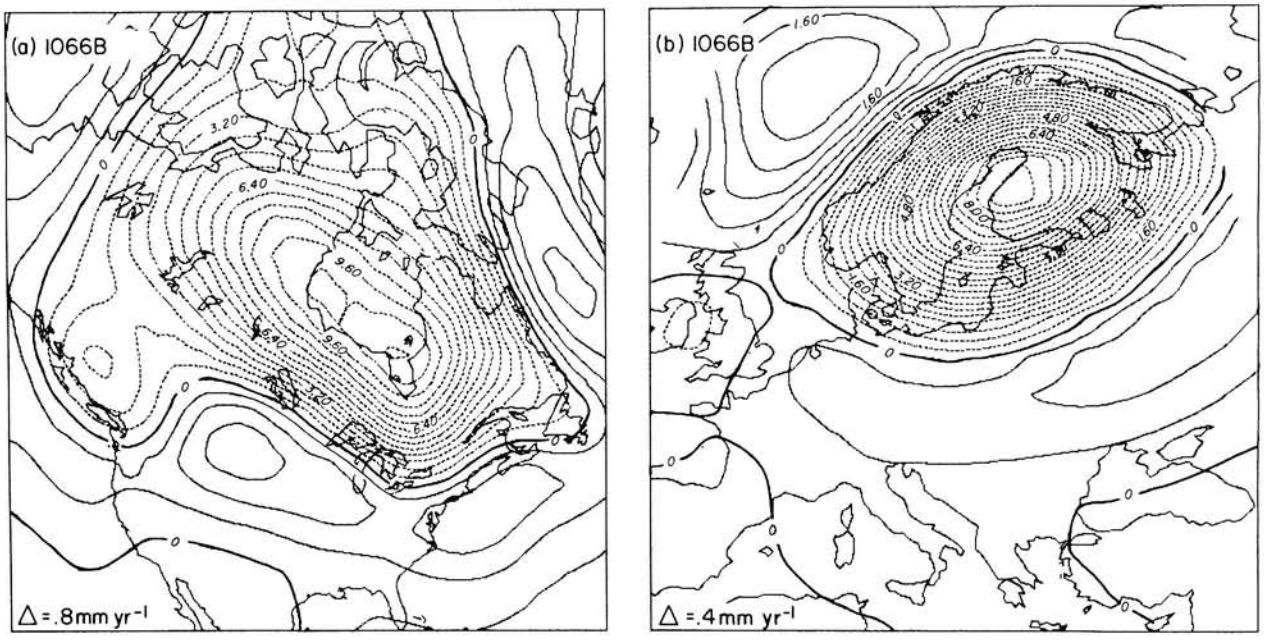

Fig. 12. Predicted rates of present-day vertical motion for (*a*) North America and (*b*) Europe based upon the model with 1066B elastic structure, lithospheric thickness of 196.6 km, upper mantle viscosity of 10^{21} Pa s, and lower mantle viscosity of 2×10^{21} Pa s. Notice the strong asymmetries in the rate of peripheral land submergence (sea level rise) in the ring-shaped regions surrounding the central regions of land emergence.

able. Because the former is a passive continental margin, whereas the latter is an active continental margin this should not be too surprising. The west coast "signal" is bound to be strongly contaminated by tectonic effects associated with the active strike-slip motion which marks the trace of the San Andreas fault. If we are interested in inferring eustatic sea level variations from the tide gauge data, we will obviously do well to avoid such regions where strong tectonic effects are known to be active. In analyzing these data we will assume that the rates listed in Tables 2*a* and 2*b* based upon the time interval

TABLE 2*a*. Tide Gauge Observed (T) and Theoretically Predicted (S) Sea Level Trends at U.S. East Coast Sites

Station (NOS Catalogue)	Place	Gamma	$(T-S)\pm E$ All Data			$(T-S)\pm E$ 1940–1980			S	T
8410140	Eastport, Maine	0.411	1.9	2.2	2.5	1.9	2.3	2.7	0.9	3.2
8418150	Portland, Maine	0.372	1.4	1.6	1.8	1.2	1.6	2.0	0.7	2.3
8419870	Seavey Island, Maine (Portsmouth, N.H.)	0.360	0.9	1.1	1.3	0.1	0.4	0.7	0.9	1.3
8443970	Boston, Mass.	0.347	0.9	1.1	1.3	−0.6	−0.3	0.0	1.2	0.9
8447930	Woods Hole, Mass.	0.336	0.8	1.0	1.2	0.3	0.6	0.9	1.7	2.3
8452660	Newport, R.I.	0.332	0.8	1.0	1.2	0.1	0.4	0.7	1.6	2.0
8454000	Providence, R.I.	0.336	−0.1	0.3	0.7	−0.1	0.3	0.7	1.5	1.8
8461490	New London, Conn.	0.325	0.4	0.7	1.0	0.4	0.7	1.0	1.5	2.2
8516990	Willets Point, N.Y.	0.306	0.2	0.6	1.0	−0.6	0.0	0.6	1.6	1.6
8518750	New York (The Battery), N.Y.	0.303	1.1	1.2	1.3	0.6	0.9	1.2	1.6	2.5
8531680	Sandy Hook, N.J.	0.300	2.2	2.5	2.8	1.9	2.3	2.7	1.7	4.0
8534720	Atlantic City, N.J.	0.280	1.7	1.9	2.1	1.4	1.8	2.2	2.1	3.9
8545530	Philadelphia, Pa.	0.286	0.6	0.8	1.0	0.0	0.5	1.0	1.8	2.3
8557380	Lewes, Del.	0.267	0.5	0.9	1.3	−0.9	−0.1	0.7	2.1	2.0
8574680	Baltimore, Md.	0.268	1.3	1.4	1.5	0.3	0.7	1.1	1.8	2.5
8575512	Annapolis, Md.	0.263	1.6	1.9	2.2	0.8	1.2	1.6	1.8	3.0
8577330	Solomons Island, Md.	0.252	1.1	1.4	1.7	0.9	1.3	1.7	1.9	3.2
8594900	Washington, D.C.	0.259	0.8	1.2	1.6	0.5	1.0	1.5	1.8	2.8
8638610	Hampton Roads (Norfolk), Va.	0.230	2.2	2.5	2.8	1.4	1.8	2.2	1.8	3.6
8638660	Portsmouth, Va.	0.228	1.6	1.9	2.2	1.5	1.9	2.3	1.7	3.6
8665530	Charleston, S.C.	0.146	2.3	2.6	2.9	1.1	1.6	2.1	0.8	2.4
8670870	Fort Pulaski (Savannah), Ga.	0.130	1.7	2.1	2.5	1.5	1.9	2.3	0.6	2.5
8720030	Fernandina Beach, Fla.	0.107	0.9	1.3	1.7	0.7	1.2	1.7	0.4	1.6
8720220	Mayport, Fla.	0.101	1.7	2.0	2.3	0.7	1.2	1.7	0.3	1.5
8723170	Miami Beach, Fla.	0.034	2.1	2.3	2.5	1.6	1.9	2.2	0.0	1.9
8724580	Key West, Fla.	0.000	2.1	2.3	2.5	1.3	1.7	2.1	−0.1	1.6

E is the standard error for the observations from the NOS catalogue. All rates are in millimeters per year.

TABLE 2*b*. Tide Gauge-Observed (T) and Theoretically Predicted (S) Sea Level Trends at U.S. West Coast Sites

Station (NOS Catalogue)	Place	Gamma	$(T-S)\pm E$ All Data			$(T-S)\pm E$ 1940–1980			S	T
9410170	San Diego, Calif.	0.000	2.1	2.2	2.3	1.5	1.9	2.3	−0.3	1.6
9410230	La Jolla, Calif.	0.004	1.8	2.0	2.2	1.4	1.8	2.2	−0.3	1.5
9410660	Los Angeles (Berth 60), Calif.	0.024	0.6	0.8	1.0	−0.3	0.1	0.5	−0.2	−0.1
9414290	San Francisco, Calif.	0.117	0.9	1.0	1.1	0.9	1.3	1.7	0.2	1.5
9414750	Alameda, Calif.	0.115	−0.6	−0.1	0.4	−0.6	−0.1	0.4	0.2	0.1
9419750	Crescent City, Calif.	0.185	−2.0	−1.7	−1.4	−2.8	−2.4	−2.0	0.8	−1.6
9439040	Astoria, Oreg.	0.252	−1.1	−0.8	−0.5	−2.1	−1.6	−1.1	0.3	−1.3
9443090	Neah Bay, Wash.	0.291	−0.9	−0.6	−0.3	−1.5	−1.1	−0.7	−0.7	−1.8
9447130	Seattle, Wash.	0.269	2.3	2.4	2.5	2.2	2.6	3.0	−0.5	2.1
9449880	Friday Harbor, Wash.	0.286	1.6	1.9	2.2	1.1	1.5	1.9	−1.0	0.5
9450460	Ketchikan, Ark.	0.432	1.4	1.6	1.8	0.8	1.3	1.8	−1.7	−0.4
9451600	Sitka, Ark.	0.478	−2.4	−2.1	−1.8	−2.5	−2.1	−1.7	−0.3	−2.4

E is the standard error for the observations from the NOS catalogue. All rates are in millimeters per year.

1940–1980 are the rates which the isostatic adjustment model should be able to predict. This is based upon the fact, evident by inspection of the data shown, that along the U.S. east coast the submergence rates based upon "all data" are generally stronger than those based upon only the last 40 years of information, indicating that the rates are generally decelerating. Since, as we shall see, the isostatic adjustment model generally predicts rates which are lower than those observed, in choosing the rates 1940–1980 as representative, we will be obtaining the best possible fit of the model to the observed rates and therefore minimizing the residual between prediction and observation.

Theoretically predicted and observed secular rates of RSL variation for both the east and west coasts of the United States are compared in Figures 13*a* and 13*b*, respectively. The residual (corrected) rates of RSL rise observed at each of the 26 tide gauges along the east coast are shown as heavy crosses which are plotted as a function of position along the coast with distance (in radians) measured positive to the north of the southernmost gauge on the coast which is located at Key West, Florida. The northernmost gauge, as shown in Table 2, is that located at Eastport, Maine. The predictions of the glacial isostatic adjustment model which were actually applied to make the correction at each tide gauge location are shown as a series of three closely spaced curves which respectively correspond to predicted rates at 18 kyear following the onset

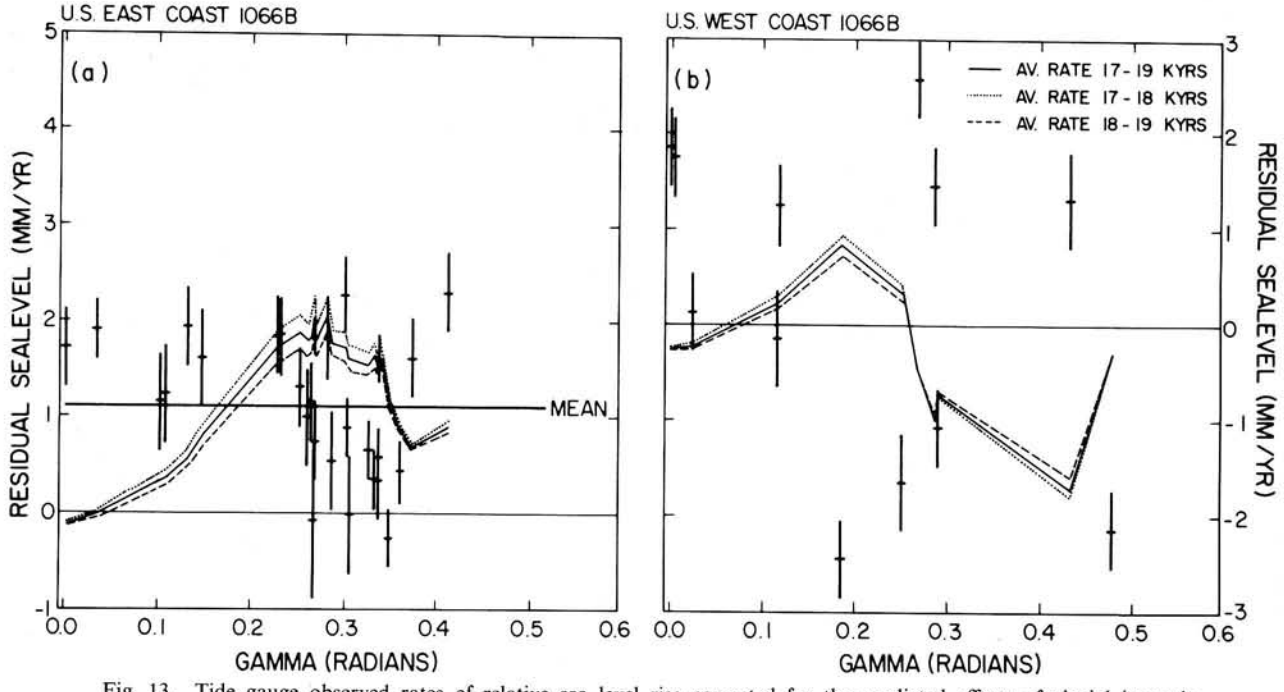

Fig. 13. Tide gauge observed rates of relative sea level rise corrected for the predicted effects of glacial isostatic adjustment based upon calculations with the same viscoelastic earth model as was employed to produce Figure 12. The corrected data are shown for both (*a*) the U.S. east coast and (*b*) the U.S. west coast. The magnitude of the correction which was applied to the raw tide gauge data varies as a function of position along the coast and is shown by the three lines labeled in the figure legend as corresponding to the three times of 17.5, 18, and 18.5 kyear. The best estimate of model present is provided by the 18-kyear curve, and this has been employed to correct the raw data. The mean of the residual rate for the U.S. east coast data is also shown but not for the west coast since the scatter in the residuals is so great that the average would not be meaningful physically.

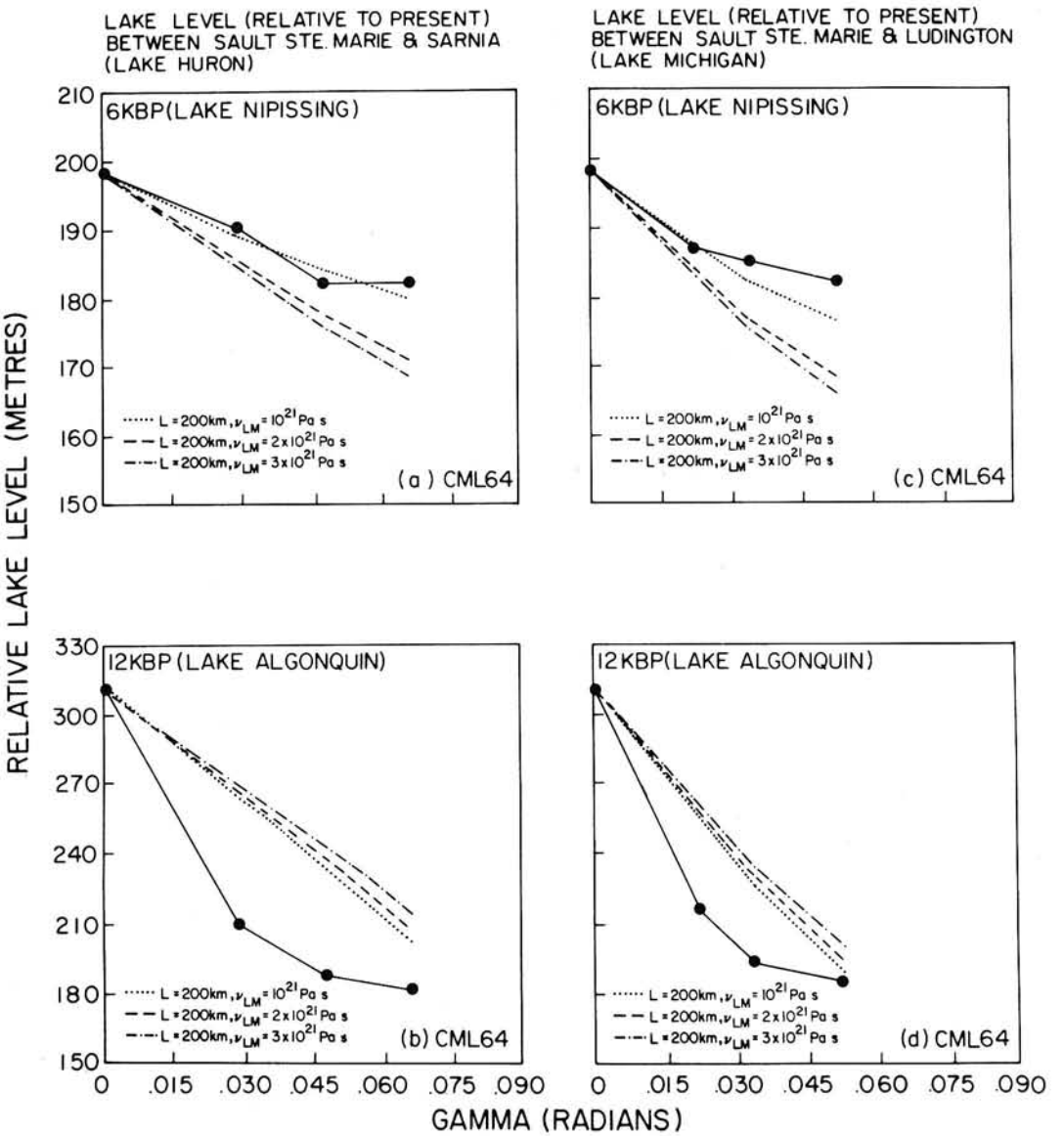

Fig. 14. Observed and predicted tilts of the Lake Nipissing (6 kyear) and Lake Algonquin (12 kyear) strandlines along traverses through Lake Huron (Figures 14*a* and 14*b*) and Lake Michigan (Figures 14*c* and 14*d*). The observations are from the compilation by *Broecker* [1966] and are shown as the solid curves. All of the predictions shown on this figure are based upon a model with simple CML64 elastic structure. The explicit locations of the Lake Huron and Michigan traverses are shown on Figure 17.

of melting (the present day in the model) and at 17.5 and 18.5 kyear to give some indication of the stability of the theoretical predication with respect to possible timing errors in the deglaciation history. Clearly, such plausible variations are rather small compared to the magnitude of the isostatic adjustment effect itself and to the rates observed. The mean of the residuals at all U.S. east coast gauges is shown by the heavy solid line marked MEAN which has a value near 1.1. mm yr^{-1} which is about 50% lower than the average which would have been obtained on the basis of the "raw" tide gauge rates listed in Table 2. It is therefore clear that the eustatic component of sea level rise which is implied by the tide gauge observations has been considerably reduced by accounting for the known influence of glacial isostatic adjustment. At three of the 26 gauges the residual is in fact very near zero, implying that all of the tide gauge observed secular sea level trend at these sites is explicable on the basis of the isostatic adjustment effect. At a further nine of the 26 gauges the corrected rates are considerably lower than the mean residual. Of greatest interest, however, is the level of scatter of the corrected rates about the mean residual rate. If there were a strong eustatic signal in the data, we would expect the corrected rates to exhibit much more modest variability about the mean than in fact obtains. This argues that there are processes contribution to the tide gauge data (e.g., river runoff, meteorological forcing through wind stress variations on the sea surface, sedimentary loading effects in the vicinity of the mouth of the Mississippi River, etc.) in excess of that which could be associated with a eustatic variation of level which might be ascribed, for example, to a presently occurring reduction of the mass bound in continental ice complexes [*Hansen et al.*, 1981; *Gornitz et al.*, 1982; *Meier*, 1984].

A parallel treatment of the observed west coast sea level trends is presented in Figure 14*b*. Again the theoretical predictions of the rate of sea level rise expected due to isostatic adjustment effects is shown for three closely spaced times

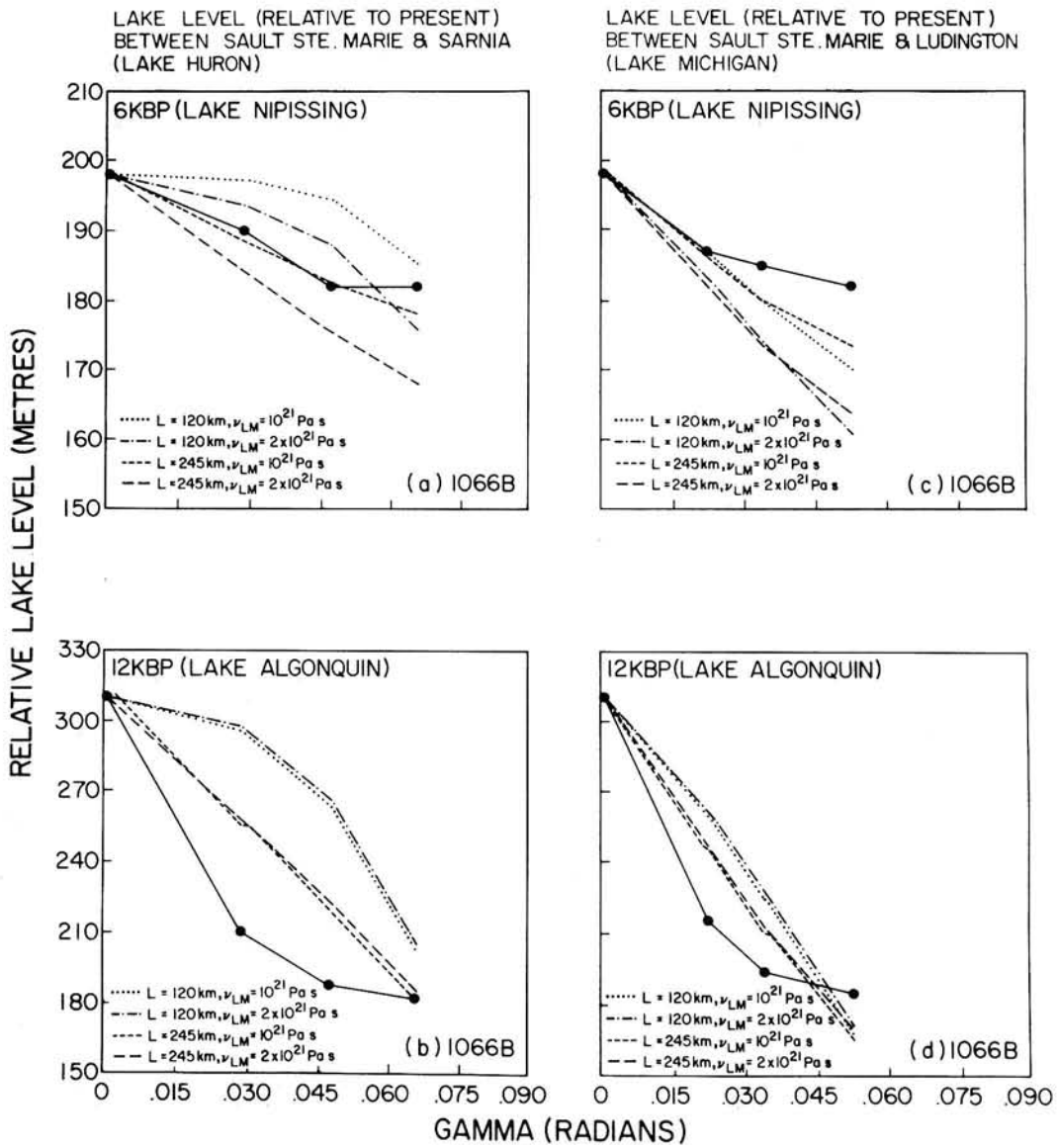

Fig. 15. Same as Figure 14 but illustrating the agreement between observations and theory for models based upon elastic structure 1066B.

(17.5, 18, 18.5 kyear following the onset of ice sheet disintegration). Again the corrected data are shown as crosses which are plotted as a function of position along the coast measured positive to the north of the southernmost tide gauge which in this case is located at San Diego. Here there is a region of positive rates of sea level rise predicted for those sites on the coast to the south of Washington State with a region of negative rates associated with the postglacial rebound induced by the melting of the Cordilleran ice complex to the north. Noticeable on this plate and on the previously described one for the U.S. east coast region are points at which the theoretically predicted rate is displaced sharply from the smoothly varying curve which would otherwise pass through the curve of predicted rate versus position along the coast. These "glitches" in the prediction are caused by the discretization error associated with the finite element method which has been employed to solve the sea level equation (see *Peltier et al.* [1978] for a description of the numerical methods employed to solve equation (17)). Most obvious by inspection of the west coast comparisons shown on Figure 13*b*, however, is the fact that the scatter of the observed rates along this coast is so extreme, both before and after correction, that no use could possibly be made of them to infer anything concerning any eustatic component of present-day RSL variation which might exist.

If there is any lesson which can be drawn from the analyses presented in this subsection of the present paper, it is certainly that great caution should be shown in attempting to infer anything about the requirement for a present-day eustatic increase of sea level on the basis of tide gauge data. If one insists on trying to do so, however, one should certainly employ data from passive continental margins in preference to those from active margins like the U.S. west coast, Japan, or the west coast of South America. Even along the U.S. east coast passive continental margin, however, the residual rates observed after the data have been corrected for isostatic adjustment effects contain strong variability as a function of position which occurs on rather small spatial scales. Considerable further work will be required to provide a complete interpretation of this information.

In the remaining sections of this paper we will focus on a

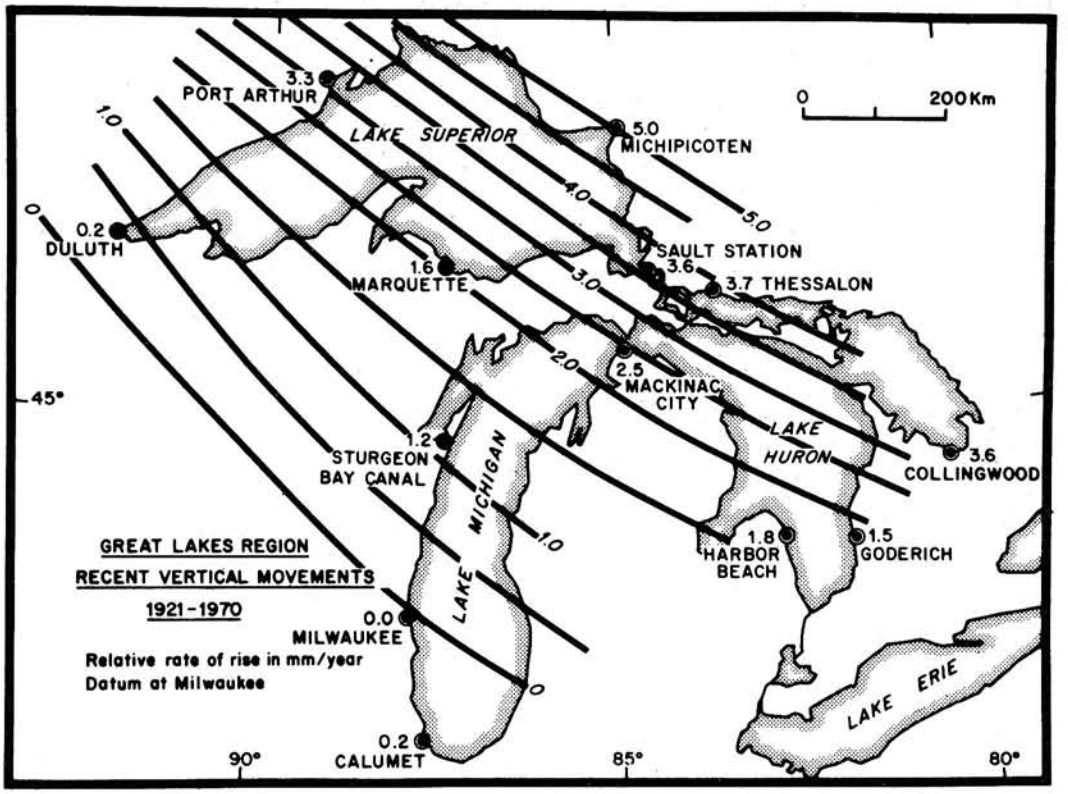

Fig. 16. Present-day rates of vertical motion through the Great Lakes region based upon the regional tide gauge network with the rates expressed relative to an arbitrary zero datum through Milwaukee [from *Walcott*, 1972].

further source of vertical motion information for the North American continent, namely, the data concerning variations of lake level in the vicinity of the Great Lakes region.

3.3. *Strandline Tilts in Proglacial Lakes: An Additional Constraint on Radial Viscoelastic Earth Structure*

Just as observed histories of relative sea level variation at discrete points on the earth's surface, as recorded in ^{14}C-controlled RSL histories or in more contemporary tide gauge observations, may be employed to usefully constrain the earth's radial viscoelastic stratification, so may the forms of single beach horizons of known age which are traceable over a sufficient surface area so as to reveal the characteristic tilt of the horizon at the location in question. Proglacial lakes are particularly useful sources of such information as they are formed at the margin the ice sheet during its retreat and often, as in the case of glacial lakes Aggasiz and Algonquin, cover a very substantial surface area. The Laurentian ice sheet of Canada was a particularly impressive creator of such lakes as evidenced by the map shown in Figure 12*a*, for example. All of the huge lakes which occur along the smooth curve extending from the Great Lakes in the southeast, to lakes Winnipeg and Manitoba on the eastern edge of the Canadian Prairie, to Great Bear and Great Slave lakes to the northwest, are proglacial lakes which lie along what was the margin of Laurentian ice at 18 kyear B.P. In these lakes it is sometimes possible to trace the position of a beach of fixed and known age around the entire circumference of the lake and to measure thereby the tilt of the ancient water plane relative to the equipotential surface defined by the present surface of the lake. Although this equipotential surface is not normally coincident with the geoid at the same location, it is, nevertheless, an equipotential and may therefore be employed as a surface against which to measure the tilting of the strandline which has been induced by the process of glacial isostatic adjustment over the time interval since the strandline was deposited.

Although some use has previously been made of such data to constrain viscoelastic earth structure, particularly lithospheric thickness by *Walcott* [1970], the models employed have been rather simple models based upon thin plate flexure theory and rather crude approximations to the actual ice sheet melting history. On this basis, Walcott inferred a lithospheric thickness of 75 km using as data the observed tilt of the Algonquin strandline which was deposited in the Great Lakes region approximately 12,000 years ago when Laurentian ice first retreated and its meltwater filled the basin. *Wolf* [1985] has recently reanalyzed this observation using a model which is only moderately more complicated than that of Walcott. His analysis has confirmed Walcott's inference and therefore served to reinforce the contradiction which exists in the literature between this estimate and the more recent one of *Peltier* [1984*a*, *b*] that was further developed in section 3.1, to the effect that U.S. east coast RSL data prefer a model with a lithospheric thickness of about 200 km (196.6 km was found to fit the observations quite well when employed in the context of a model with 1066B elastic structure and upper and lower mantle viscosities of 10^{21} Pa s and 2×10^{21} Pa s, respectively). The difference by almost a factor of 3 between these estimates of lithospheric thickness should be explicable. What I will do here is to reinterpret strandline tilt data from the Great lakes region using the same gravitationally self-consistent model of the isostatic adjustment process as has been employed to reconcile the previously discussed observations. As we will see, when the more accurate model is employed, the tilt observations then accept the same increased

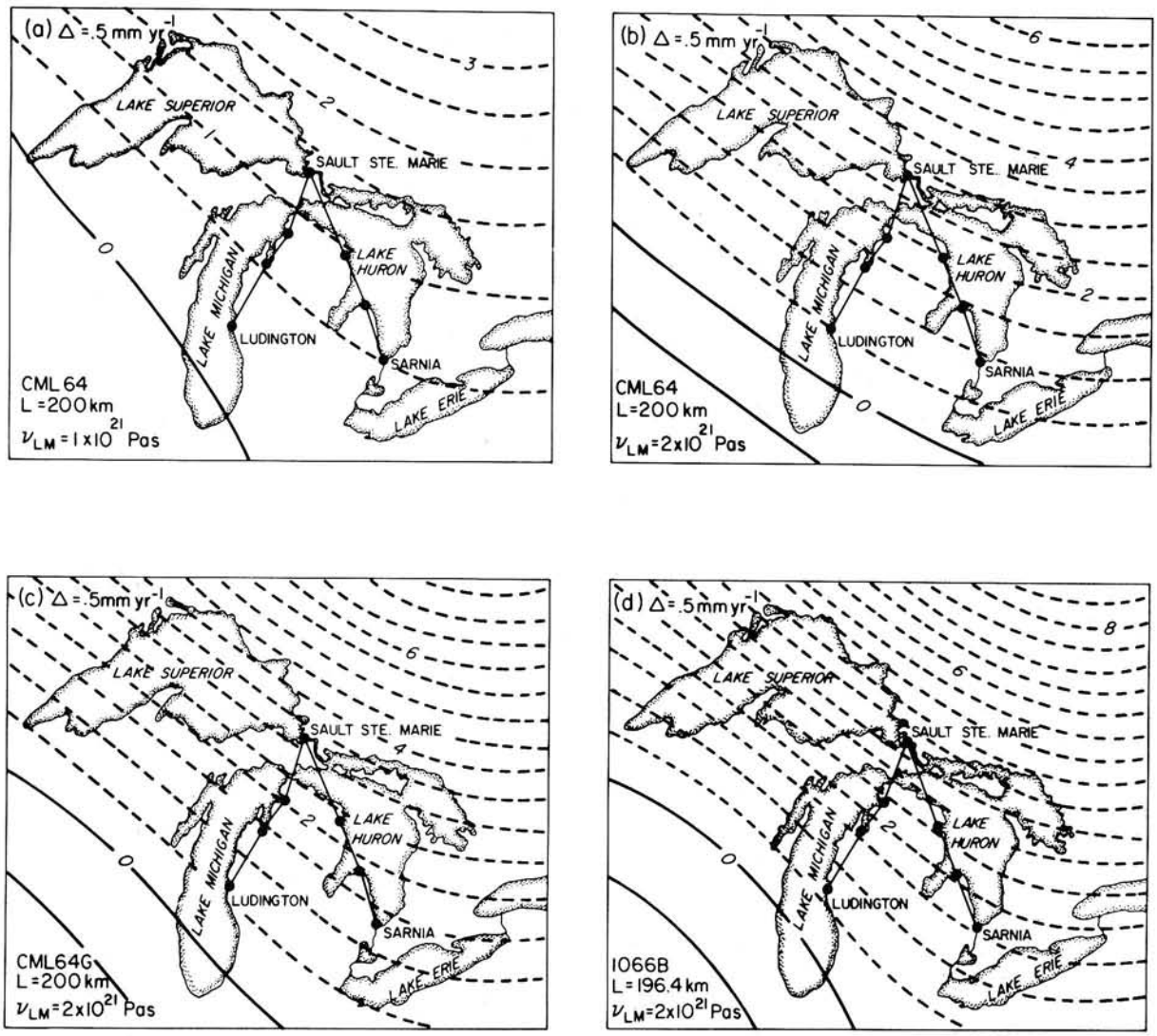

Fig. 17. Maps of the rate of vertical motion predicated for the Great Lakes region adjusted to a reference datum through Milwaukee for comparisons with the observed data shown on Figure 16. All calculations are based on models which have lithospheric thicknesses of 200 km. Figures 17*a* and 17*b* are predictions for models which have the simple CML64 elastic structure. (*a*) For the model with a uniform mantle viscosity of 10^{21} Pa s. (*b*) For the model which has an upper mantle viscosity of 10^{21} Pa s and a lower mantle viscosity of 2×10^{21} Pa s. (*c*) The predicted variation of the present-day rate of vertical motion for the model with elastic structure CML64G. (*d*) For model 1066B. Both of the latter calculations are for models which have the same viscous structure as that employed to compute the result shown in Figure 17*b*. Comparison of the prediction in Figure 17*d* with the observed map shown in Figure 16 demonstrates excellent agreement.

lithospheric thickness as is required by the east coast RSL data. The source of tilt observations which we will employ is the compilation by *Broecker* [1966] and discussed in greater detail with respect to coverage of the early literature by *Walcott* [1972].

Our results from this analysis are illustrated by Figures 14 and 15 which respectively show calculations of the form of the Lake Nipissing (6 kyear B.P.) and Lake Algonquin (12 kyear B.P.) strandlines predicted by the model on respective traverses through lakes Huron and Michigan (the locations of these traverses are shown on Figure 17). On each plate the solid curve represents the observations along such representative traverses, while the other curves represent predictions of the theoretical model. For each strandline the observed height at Sault St. Marie is taken as the reference height, and the theoretical predictions are adjusted to agree with the observations at this point. There is clearly sufficient freedom in the physics to allow this as rather considerable variations of absolute water amount in the lakes are expected to have occurred both during and subsequent to completion of the deglaciation process. Focusing first on the comparisons shown on Figure 14, which are all for models with a fixed lithospheric thickness of 200 km and CML64 elastic structure, we note that the data are best fit by models with a lower mantle viscosity of 10^{21} Pa s, which is equal to the assumed upper mantle value. In general, however, the observed form of the Algonquin strandline is not well explained by the model, as the observations show considerably greater curvature than the theoretical predictions with much shallower tilts obtaining to the south than to the north at Sault St. Marie where they are rather steep. If the lithosphere has a thickness of 200 km as the east coast RSL data have been taken to imply, the

viscosity of the mantle must be uniform and an increase by even a factor of 2 substantially degrades the fit of the model to the data.

The trade-off between variations of lithospheric thickness and variations of lower mantle viscosity which was shown to be important with respect to understand east coast RSL data is explored in the context of the proglacial lake strandline tilt observations in terms of calculations using 1066B elastic structure in Figure 15. Here predictions of the same observations are shown for four different earth models which differ only in their values of ν_{LM} and L which are assumed to have either one or the other of the respective pairs of value (10^{21} Pa s, 2×10^{21} Pa s) and (120 km, 245 km). These comparisons show that the steep tilt of the Lake Algonquin beaches is best fit by the thick lithosphere models whereas for the thick lithosphere model to simultaneously fit the much shallower tilts of Lake Nipissing beaches the uniform mantle viscosity of 10^{21} Pa s is required. Increasing the lower mantle viscosity to the value of 2×10^{21} Pa s leads to the prediction of excessive present-day tilting of the Nipissing beaches. Clearly, the lithospheric thickness must be reduced to a value less than 245 km (say 200 km) in order to accommodate the $\times 2$ increase of lower mantle viscosity preferred to east coast RSL data. Comparing these results based on the 1066B model with those described in connection with Figure 14 based on model CML64 again demonstrates that the amount of deformation realized with a seismically "realistic" model like 1066B is greater than that realized with the less "realistic" CML64 model so that greater lithospheric thickness may be tolerated in the model to achieve a given level of deformation. These calculations suffice to show that the extremely thin lithosphere obtained by Walcott is a consequence of his having used an overly simplified parameterization of the radial viscoelastic structure. In order to further improve our estimates of this parameter using the strandline tilt data will require a much more accurate unloading history in this region than that embodied in the ICE-2 representation of *Wu and Paltier* [1983]. For example, the reversed tilts delivered by the thin lithosphere models for the Lake Huron traverse are due to edge effects associated with low resolution of the ice history in which the edges of individual finite elements become apparent. We will have to rectify this shortcoming in later work.

3.4. *Tide Gauge Observations of Differential Rates of Vertical Motion Across the Great Lakes Region: A Further Observational Datum*

One further set of observations which relate to deglaciation-induced vertical motions of the North American continent which we will consider in this paper are again concerned with tide gauge data. In this case, however, we will consider tide gauge observations of the "present-day" rate of vertical motion across the entire Great Lakes region as these define a surface of spatial variations in rate such as that which we previously discussed on the scale of the entire North American and European continents. Figure 16 shows a reproduction, from *Walcott* [1972], of a map of tide gauge observed rates of vertical motion relative to a zero rate assumed for Milwaukee. This shows that the observed differential rate of land emergence between Milwaukee and the northern edge of the Great Lakes is near 5 mm yr^{-1}, and this is the observation which we would like to reproduce with the theoretical model.

The success of the model in reproducing this observation is established in Figure 17 which shows maps of the predicted present-day rate of vertical motion which have been adjusted to a reference level of zero rate for Milwaukee as in the presentation of the observations by *Walcott* [1972] shown in Figure 16. Predicted maps are shown for a sequence of models with elastic structures described in Table 1 and with fixed lithospheric thickness of 200 km. The first two calculations make use of elastic structure CML64 and demonstrate the effect on the predictions of increasing the lower mantle viscosity by a factor of 2 from 10^{21} Pa s in Figure 17*a* to 2×10^{21} Pa s in Figure 17*b*. Clearly, increasing the deep mantle viscosity by even this small factor substantially increases the predicted present-day rates of emergence and greatly improves the fit of the predicted map to the observed. Without this modest increase of lower mantle viscosity the predicted rates are more than a factor of 2 too low. However, even this modification still leaves the theoretical prediction with too little differential in the rate of vertical motion across the Great Lakes. A further significant improvement of the fit of the theory to the observation is obtained in Figure 17*c* which is based upon a calculation which uses model CML64G for the elastic structure. As shown in Table 1, this model includes not only the full effects of compressibility throughout the mantle but also a substantial increase of internal buoyancy to better match the magnitude of this effect which is delivered by model 1066B. Although this calculation again takes the theoretical prediction closer to the observations, the differential rate of vertical motion across the Great Lakes is still somewhat smaller than the observed differential. Figure 17*d* shows the map predicted using 1066B elastic structure. This map is in almost exact accord with the observations and further demonstrates the degree to which even the detailed "fine structure" of the postglacial rebound process may be reconciled with the extremely simple model of the radial viscoelastic structure upon which we have settled in the process of the present refinement of past analyses. Most of the observations "like" the simple Maxwell model with a lithospheric thickness near 200 km, an upper mantle viscosity of 10^{21} Pa s, and a lower mantle viscosity about a factor of 2 in excess of the upper mantle value. Some of the observations, most notably free air gravity anomalies which have not been discussed here, also seem to require the presence of some internal buoyancy in the mantle [e.g., *Peltier and Wu*, 1982; *Wu and Peltier*, 1983; *Peltier*, 1985*a*, *b*]. In the following section we will comment upon the conclusions which should be drawn from this in the light of the comment made in the introduction concerning the possible importance of transient rheology to the postglacial rebound phenomenon.

4. CONCLUSIONS

One of the most important new results which have been obtained in the present paper concerns the refinement of the constraints on deep mantle viscosity and lithospheric thickness which were obtained in previous investigations with the same theory as employed here. RSL data from the U.S. east coast require a small increase of lower mantle viscosity to a value near 2×10^{21} Pa s in order to fit the submergence curve for Florida. Without this slight viscosity increase, raised beaches are predicted for Florida which are not observed. However, a strong upper bound upon the viscosity increase is proved from RSL data on the northern flank of the glacial forebulge. An increase of lower mantle viscosity to a value in excess of 2×10^{21} Pa s removes the nonmonotonic form of the RSL prediction which is required to fit the data because

this modification of the model prevents the migration of the bulge which is required to produce this signature in the response. The slight increase of lower mantle viscosity also has a salutory effect on the fits to some RSL data from within the ice margins. When the lower mantle viscosity is fixed to the value of 2×10^{21} Pa s, then east coast RSL data require a lithospheric thickness of about 200 km in order to explain the submergence observed over the crest of the forebulge which is located in the vicinity of New York City along the U.S. east coast.

We applied this viscoelastic model to filter from the tide gauge observed rates of RSL rise along the U.S. east coast, the signal due to the collapsing forebulge. After filtering, the average of residual rates of rise was reduced to about 1.1 mm yr^{-1} which is considerably less than the 1.5 mm yr^{-1} rate which has often been assumed to be representative of the eustatic component and about which a great deal of interest has been recently expressed in the context of discussions of the possible climatic implications of this eustatic component. In fact the reduced average is very close to that which *Gornitz et al.* [1982] and, following them, *Meier* [1984] have accepted as the possible contribution to the tide gauge inferred secular change due to steric effects (that is to the increase of RSL which might be explained as a consequence of thermal expansion of the oceans). Only to the extent that observed eustatic RSL rise is not explicable in terms of steric effects is it necessary to invoke an increase in ocean mass due to the melting of continental ice sheets and glaciers. The theoretical model which we have applied here to filter the North American data should next be applied to the same global data set as has recently been analyzed by *Barnett* [1983]. It will be interesting to see whether any significant nonsteric component remains after this global analysis is performed. These calculations are presently ongoing and the results obtained from them will be reported in due course.

Two further data sets have also been integrated into this program of analysis of glaciation-induced deformations, the first of these are observations of strandline tilts in proglacial lakes which were previously employed by *Walcott* [1970] in support of the notion that the thickness of the continental lithosphere was rather thin and near 75 km. We have shown that this small inferred value for the lithospheric thickness was due to his use of an overly simplistic parameterization of the radial viscoelastic structure. When a more realistic parameterization of this structure is employed, these data are found to be compatible with the same thickness near 200 km which is required by east coast RSL observations. Tide gauge observations of present-day vertical motion across the Great Lakes region were also shown to accord nicely with the same model of the radial structure when the ICE-2 melting history of *Wu and Peltier* [1983] is employed to make the predictions. These data have not previously been predicted by any model of the glacial rebound process.

Probably most significant of all of the analyses presented here, however, concerns the interpretation of the rather low value of the viscosity of the lower mantle which has been shown to be required by the totality of glacial rebound observations. If the recent conclusions of *Hager* [1984] concerning the radial variation of the steady state viscosity which is required to explain large spatial scale anomalies in the gravitational field are correct, then the lower mantle viscosity deduced from the rebound data ($\sim 2 \times 10^{21}$ Pa s) must represent a transient component of the viscosity spectrum rather than a steady state value. In section 2 of this paper I invoked the three-dimensional Burgher's body rheology introduced by *Peltier et al.* [1981] to show that this is a simply understandable scenario. If the shear modulus μ_2 of the Kelvin-Voight element of the Burgher's body is such that $\mu_2 \ll \mu_1$, then the Burgher's body degenerates to a Maxwell analogue with effective viscosity $\nu_{\text{eff}} = \nu_1\nu_2/\nu_1 + \nu_2$ so that if the transient viscosity of the Kelvin-Voight element ν_2 is such that $\nu_2 \ll \nu_1$, then the lower mantle viscosity inferred by applying the Maxwell analogue will be equal to the transient value ν_2. This will provide a rather simple means of interpreting the recent results obtained from calculations of the geoid height anomalies to be expected on the basis of seismically inferred models of the lateral heterogeneity of density in the mantle if these results should be verified by independent analyses. This idea is explored in much more detail by *Peltier* [1985*c*] and *Peltier et al.* [1985].

Acknowledgments. The research described in this paper was supported by NSERC grant A9627. I am indebted to Rosemary Drummond for her assistance with the numerical calculations and to Ana Sousa for "processing the words."

REFERENCES

Backus, G. E., Converting vector and tensor equations to scalar equations in spherical co-ordinates, *Geophys. J. R. Astron. Soc.*, *13*, 71, 1967.

Barnett, T. P., Possible changes in global sea level and their causes, *Clim. Change*, *5*(1), 15–38, 1983.

Biot, M. A., Theory of stress-strain relations in anisotropic viscoelasticity and relaxation phenomena, *J. Appl. Phys.*, *25*(1), 1385, 1954.

Broecker, W. S., Glacial rebound and the deformation of the shorelines of proglacial lakes, *J. Geophys. Res.*, *71*, 4777–4783, 1966.

Clark, J. A., W. E. Farrell, and W. R. Peltier, Global changes in postglacial sea level: A numerical calculation, *Quat. Res.*, *9*, 265–287, 1978.

Dziewonski, A. M., Mapping the lower mantle: determination of lateral heterogeneity of *P* velocity up to degree and order 6, *J. Geophys. Res.*, *89*, 5929–5952, 1984.

Dziewonski, A. M., and D. L. Anderson, Preliminary reference earth model, *Phys. Earth Planet. Inter.*, *25*, 297–356, 1981.

Farrell, W. E., and J. A. Clark, On postglacial sea level, *Geophys. J. R. Astron. Soc.*, *46*, 647–667, 1976.

Gilbert, F., and A. M. Dziewonski, An application of normal mode theory to the retrieval of structural parameters and source mechanisms from seismic spectra, *Philos. Trans. R. Soc., Ser. A*, *276*, 187–269, 1975.

Gornitz, V., L. Lebedeff, and J. Hansen, Global sea level trend in the past century, *Science*, *215*, 1611–1614, 1982.

Hager, B. H., Subducted slabs and the geoid: Constraints on mantle rheology and flow, *J. Geophys. Res.*, *89*, 6003–6015, 1984.

Hansen, J., D. Johnson, A. Lacis, S. Lebedeff, P. Lee, D. Reid, and G. Russell, Climate impact of increasing atmospheric carbon dioxide, *Science*, *213*, 957–966, 1981.

Longman, I. M., A Green's function for determining the deformation of the earth under surface mass loads, 2, Computations and numerical results, *J. Geophys. Res.*, *68*, 485–496, 1963.

Meier, M. F., Contribution of small glaciers to global sea level, *Science*, *226*, 1418–1421, 1984.

National Ocean Service, Sea level variations for the United States 1855–1980, U.S. Dep. of Commer., Nat. Oceanic and Atmos. Admin., Rockville, Md., 1983.

Peltier, W. R., The impulse response of a Maxwell earth, *Rev. Geophys.*, *12*, 649–669, 1974.

Peltier, W. R., Glacial isostatic adjustment, II, The inverse problem, *Geophys. J. R. Astron. Soc.*, *46*, 669–706, 1976.

Peltier, W. R., Mantle convection and viscosity, in *Physics of the Earth's Interior* edited by A. M. Dziewonski and E. Boschi, pp. 362–431, North-Holland, Amsterdam, 1980.

Peltier, W. R., Ice age geodynamics, *Annu. Rev. Earth Planet. Sci.*, *9*, 199–225, 1981.

Peltier, W. R., Dynamics of the ice age earth, *Adv. Geophys.*, *24*, 1–146, 1982.

Peltier, W. R., Constraint on deep mantle viscosity from LAGEOS acceleration data, *Nature, 304*, 434–436, 1983.

Peltier, W. R., The rheology of the planetary interior, *Rheology, 28*, 665–697, 1984*a*.

Peltier, W. R., The thickness of the continental lithosphere, *J. Geophys. Res., 89*, 11,303–11,316, 1984*b*.

Peltier, W. R., The LAGEOS constraint on deep mantle viscosity: Results from a new normal mode method for the inversion of viscoelastic relaxation spectra, *J. Geophys. Res., 90*, 9411–9421, 1985*a*.

Peltier, W. R., Mantle convection and viscoelasticity, *Annu. Rev. Fluid Mech., 17*, 561–608, 1985*b*.

Peltier, W. R., New constraint on transient lower mantle rheology and internal mantle buoyancy from glacial rebound data, *Nature, 318*, 614–617, 1985*c*.

Peltier, W. R., and J. T. Andrews, Glacial isostatic adjustment, I, The forward problem, *Geophys. J. R. Astron. Soc., 46*, 605–646, 1976.

Peltier, W. R., and P. Wu, Mantle phase transitions and the free air gravity anomalies over Fennoscandia and Laurentia, *Geophys. Res. Lett., 9*, 731–734, 1982.

Peltier, W. R. and P. Wu, Continental lithospheric thickness and deglaciation induced true polar wander, *Geophys. Res. Lett., 10*, 181–184, 1983.

Peltier, W. R., W. E. Farrell, and J. A. Clark, Glacial isostasy and relative sea level: A global finite element model, *Tectonophysics, 50*, 81–110, 1978.

Peltier, W. R., P. Wu, and D. A. Yuen, The viscosities of the earth's mantle, in *Anelasticity in the Earth*, Geodyn. Ser., vol. 4, edited by F. D. Stacey, M. S. Paterson, and A. Nicholas, pp. 59–77, AGU, Washington, D. C., 1981.

Peltier, W. R., R. Drummond, and M. Tushingham, Postglacial rebound and transient lower mantle rheology, *Geophys. J. R. Astron. Soc.*, in press, 1986.

Sammis, C. G., J. C. Smith, G. S. Schubert and D. A. Yuen, Viscosity depth profile of the earth's mantle: Effects of polymorphic phase transitions, *J. Geophys. Res., 82*, 3747–3761, 1977.

Walcott, R. I., Flexural rigidity, thickness and viscosity of the lithosphere, *J. Geophys. Res., 75*, 3941–3954, 1970.

Walcott, R. I., Late Quaternary vertical movements in Eastern North America: quantitative evidence of glacio-isostatic rebound, *Rev. Geophys., 10*, 849–884, 1972.

Weertman, J., Creep laws for the mantle of the earth, *Philos. Trans. R. Soc. London, Ser. A, 288*, 9–26, 1978.

Wolf, D., An improved estimate of lithosphere thickness based on a re-interpretation of tilt data from Pleistocene Lake Algonquin, *Can. J. Earth Sci.*, in press, 1985.

Woodhouse, H. J., and A. M. Dziewonski, Mapping the upper mantle: Three-dimensional modeling of earth structure by inversion of seismic waveforms, *J. Geophys. Res., 89*, 5953–5986, 1984.

Wu, P. and W. R. Peltier, Glacial isostatic adjustment and the free air gravity anomaly as a constraint on deep mantle viscosity, *Geophys. J. R. Astron. Soc., 74*, 377–449, 1983.

Wu, P., and W. R. Peltier, Pleistocene deglaciation and the earth's rotation: A new analysis, *Geophys. J. R. Astron. Soc., 76*, 202–242, 1984.

Yoder, C. F., J. G. Williams, J. O. Dickey, B. E. Schultz, R. J. Eanes, and B. D. Tapley, Secular variation of earth's gravitational harmonic J_2 coefficient from LAGEOS and nontidal acceleration of earth rotation, *Nature, 303*, 757–762, 1983.

Yuen, D. A., and W. R. Peltier, Normal modes of the viscoelastic earth, *Geophys. J. R. Astron. Soc., 69*, 495–526, 1982.

W. R. Peltier, Department of Physics, University of Toronto, Toronto, Ontario, Canada M5S 1A7.

(Received July 1, 1985;
revised November 22, 1985;
accepted December 3, 1985.)